Scaling and predicting solute transport processes in streams

Ricardo González-Pinzón,[1] Roy Haggerty,[1] and Marco Dentz[2]

Received 27 September 2012; revised 11 April 2013; accepted 29 April 2013.

[1] We investigated scaling of conservative solute transport using temporal moment analysis of 98 tracer experiments (384 breakthrough curves) conducted in 44 streams located on five continents. The experiments span 7 orders of magnitude in discharge (10^{-3} to 10^{3} m^3/s), span 5 orders of magnitude in longitudinal scale (10^{1} to 10^{5} m), and sample different lotic environments—forested headwater streams, hyporheic zones, desert streams, major rivers, and an urban manmade channel. Our meta-analysis of these data reveals that the coefficient of skewness is constant over time (CSK $= 1.18 \pm 0.08$, $R^2 > 0.98$). In contrast, the CSK of all commonly used solute transport models decreases over time. This shows that current theory is inconsistent with experimental data and suggests that a revised theory of solute transport is needed. Our meta-analysis also shows that the variance (second normalized central moment) is correlated with the mean travel time ($R^2 > 0.86$), and the third normalized central moment and the product of the first two are very strongly correlated ($R^2 > 0.96$). These correlations were applied in four different streams to predict transport based on the transient storage and the aggregated dead zone models, and two probability distributions (Gumbel and log normal).

Citation: González-Pinzón, R., R. Haggerty, and M. Dentz (2013), Scaling and predicting solute transport processes in streams, *Water Resour. Res.*, *49*, doi:10.1002/wrcr.20280.

1. Introduction

[2] Two of the most challenging problems in surface hydrology are scaling and predicting solute transport in streams [*Young and Wallis*, 1993; *Jobson*, 1997; *Wörman*, 2000; *O'Connor et al*., 2010]. We must resolve these challenges to wisely manage water resources because there is a need to understand controls on stream ecosystems at local, regional, and continental scales, and because we need to predict transport in environments and conditions that do not have supporting tracer test data.

[3] Quantitative representations of hydrobiogeochemical processes are based on mathematical and numerical simplifications. Each simplification, the need to parameterize and integrate spatial and temporal processes, and the limitation of available observations to constrain models introduce structural errors and uncertainty in the predictions derived from such models [*Beven*, 1993; *Wagener et al*., 2004]. On the other hand, the transferability of empirical relationships from intensely instrumented catchments (mainly located in developed countries) to ungauged catchments relies on the similarity of hydrobiogeochemical characteristics [*Sivapalan*, 2003], thus limiting their practical application in regions where they are more needed.

[4] Solute transport and nutrient processing have been analyzed from different modeling perspectives, i.e., physically based, stochastic [*Botter et al*., 2010; *Cvetkovic et al*., 2012] and data-based mechanistic approaches [*Young and Wallis*, 1993; *Young* 1998; *Ratto et al*., 2007]. Although these approaches have increased our awareness about key compartments and hydrologic conditions that exert important influence on biogeochemical processes, i.e., identification of hot spots and hot moments [*McClain et al*., 2003], there is not yet a unified approach that has proven successful to scale and predict solute transport and nutrient processing.

[5] In the last three decades, research on solute transport and nutrient processing has revealed complex interactions between landscape and stream ecosystems, and attempts to scale and predict these processes have been limited by the difficulty of measuring and extrapolating hydrodynamic and geomorphic characteristics [*Scordo and Moore*, 2009; *O'Connor and Harvey*, 2008; *O'Connor et al*., 2010], and by the qualitatively confusing analyses derived from poorly constrained parametric interpretations of model-based approaches. A literature review presented hereafter (chronologically organized) shows contradictory evidence about the relationship between transient storage (TS) [*Bencala and Walters*, 1983; *Beer and Young*, 1983], the theory most frequently used to explain solute transport and in-stream processing. *Valett et al*. [1996] found a strong correlation ($R^2 = 0.77$) between TS and NO_3 retention in three first-order streams in New Mexico. *Mulholland et al*. [1997] found larger PO_4 uptake rates in a stream with higher TS, when they compared two forested streams. *Martí et al*. [1997] found no correlation between NH_3

[1]College of Earth, Ocean, and Atmospheric Sciences, Oregon State University, Corvallis, Oregon, USA.
[2]Department of Geosciences, Institute of Environmental Assessment and Water Research (IDAEA-CSIC), Barcelona, Spain.

Corresponding author information: R. González-Pinzón, College of Earth, Ocean, and Atmospheric Sciences, 104 Wilkinson Hall, Oregon State University, Corvallis (OR), 97331-5506, USA. (gonzaric@geo.oregonstate.edu)

0043-1397/13/10.1002/wrcr.20280

uptake length and A_s/A (TS to main channel sizing ratio) in a desert stream. *Hall et al*. [2002] found a very weak correlation ($R^2 = 0.14 - 0.35$) between TS parameters and NH_4 demand in Hubbard Brook streams. In the 11 stream LINX-I data set, *Webster et al*. [2003] found no statistically significant relationship between NH_4 uptake and TS. *Thomas et al*. [2003] showed that TS accounted for 44%–49% of NO_3 retention measured by ^{15}N in a small headwater stream in North Carolina. *Niyogi et al*. [2004] did not find significant correlations among soluble reactive phosphorous (P-SRP) and NO_3 uptake velocities, and TS parameters. *Ensign and Doyle* [2005] found an increase of A_s/A and uptake velocities for NH_4 and PO_4, after the addition of flow baffles to the streams studied. *Ryan et al*. [2007] found strong relationships in two urban streams between P-SRP retention and TS when the variables were measured at different regimes in the same stream. *Lautz and Siegel* [2007] found a modest correlation ($R^2 = 0.44$) between NO_3 retention efficiency and TS in the Red Canyon Creek watershed (WY). *Bukaveckas* [2007] reported an indefinite relationship between TS and NO_3 and P-SRP retention efficiencies. Lastly, the LINX-II data set from ^{15}N-NO_3 injections in 72 streams showed no relationship between NO_3 uptake and TS [*Hall et al*., 2009].

[6] One factor that might contribute to the absence of strong relationships between TS and nutrient processing is the use of metrics that obscure the importance of TS across study sites (see discussions by *Runkel* [2002, 2007]). Also, it has become apparent that there are important limitations to identifying TS parameters with current techniques [*Wagener et al*., 2002; *Schmid*, 2003; *Camacho and González-Pinzón*, 2008], i.e., multiple sets of parameters might represent field observations "equally well" [*Beven and Binley*, 1992], and choosing a unique set of parameters to describe the behavior of a system might lead to misinterpretations of their physical meaning (if any), especially when those parameter sets are used to compare streams from different ecosystems and/or hydrologic conditions.

[7] In spite of the observed complexity of solute transport processes in streams, it is surprising that systems governed by physical processes that are considered "well understood" and by reasonably predictable biochemical interactions behave so unpredictably when combined. More robust methods are required to deconvolve signal imprints of solute transport and nutrient processing, thus allowing the development and implementation of improved decision-making approaches for stream management.

[8] In this paper, we investigated the existence of temporal patterns that can be used to scale and predict solute transport processes using an extensive database of tracer experiments that span 7 orders of magnitude in discharge, 5 orders of magnitude in longitudinal scale, and sample different lotic environments on five continents–forested headwater streams, hyporheic zones, desert streams, major rivers, and an urban manmade channel. From this meta-analysis, which is only implicitly dependent on hydrogeomorphic characteristics, we have proposed an approach to perform uncertainty analysis on solute transport processes and discussed some inconsistencies of the classic solute transport theory.

2. Methodology

2.1. Temporal Moments From Time Series

[9] We investigated conservative solute transport using temporal moments of the histories of multiple conservative tracer tests. Our analysis is based on an Eulerian approach, where the time series have been collected at different fixed spatial locations in each stream. Temporal moments have been widely used in the study of solute transport and biochemical transformations. *Das et al*. [2002] and *Govindaraju and Das* [2007] presented an extensive review of the theory and applications of temporal moment analysis to study the fate of conservative and reactive solutes. Recently, *Leube et al*. [2012] discussed the efficiency and accuracy of using temporal moments for the physically based model reduction of hydrogeological problems.

[10] Moments of distributions are commonly expressed as measures of central tendency. The nth absolute moment (also referred to as the nth raw moment or nth moment about 0), μ_n, of a concentration time series, $C(t)$, is defined as

$$\mu_n = \int_0^\infty t^n C(t)\mathrm{d}t \tag{1}$$

[11] The nth normalized absolute moment (also referred to as the nth normalized raw moment or nth normalized moment about 0), μ_n^*, is defined as

$$\mu_n^* = \frac{\mu_n}{\mu_0} \tag{2}$$

and the nth normalized central moment (also referred to as the nth normalized moment about the mean), m_n, is defined as

$$m_n = \frac{1}{\mu_0}\int_0^\infty \left(t - \mu_1^*\right)^n C(t)\mathrm{d}t \tag{3}$$

$$m_n = \sum_{i=0}^{n} \binom{n}{i} \mu_{n-i}^* \left(-\mu_1^*\right) i \tag{4}$$

where i is an index. Note that (4) is an inverse binomial transform that can be easily used to calculate the normalized central moments of order 1 (mean travel time), 2 (variance), and 3 (skewness):

$$\begin{aligned} m_1 &= \mu_1^* \\ m_2 &= \mu_2^* - \mu_1^{*2} \\ m_3 &= \mu_3^* - 3\mu_1^*\mu_2^* + 2\mu_1^{*3} \end{aligned} \tag{5}$$

[12] Temporal moments are also related to residence time distributions and transfer functions of linear dynamic systems [*Jury and Roth*, 1990; *Sardin et al*., 1991]. *Aris* [1958] developed a method to compute the theoretical temporal moments of linear functions, thus allowing the use of experimental temporal moments (i.e., those estimated from observed time series) to estimate the parameters of linear dynamic models, i.e.,

$$\mu_n = (-1)^n \lim_{s\to 0}\left\{\frac{d^n}{\mathrm{d}s^n}\left[\overline{C}(x,s)\right]\right\} \tag{6}$$

where $\overline{C}(x,s)$ is the Laplace transform of $C(x,t)$ and x is the longitudinal distance in one-dimensional approximations.

[13] Theoretical temporal moments for most solute transport models have been estimated for different types of boundary conditions. A few examples of the progress on

this topic are the development of temporal moment-generating equations to model transport and mass transfer [*Harvey and Gorelick*, 1995; *Luo et al*., 2008], and the calculation of temporal moments for the TS model [*Czernuszenko and Rowinski*, 1997; *Schmid*, 2002], equilibrium and nonequilibrium sorption models [*Goltz and Roberts*, 1987; *Cunningham and Roberts*, 1998], the aggregated dead zone model [*Lees et al*., 2000], and the metabolically active TS model [*Argerich et al*., 2011].

[14] Matching (or equating) experimental and theoretical temporal moments is a useful technique to parameterize linear models [*Nash*, 1959]. The advantages of using experimental moments to match theoretical moments come with the challenge to completely recover the tracer experiment signals, as it has been shown that truncation errors affect the estimation of higher-order temporal moments. Using experimental data, *Das et al*. [2002] and *Govindaraju and Das* [2007] showed that when the error in mass recovery is 16%, the errors in absolute *n*th moments can be as high as approximately $(n+1)\cdot 16\%$ for $n=0$ through $n=4$. This problem is related to the early cutoff of data measurement or the lack of instrumental resolution to detect low concentrations of tracers, and is not related to the apparent incomplete mass recovery due to dilution effects (e.g., groundwater contributions). Note that correcting the observed breakthrough curves (BTCs) uniformly (with a steady-state gain factor) for dilution only affects the magnitude of the absolute moments but does not modify the magnitude of the normalized absolute moments or that of the normalized central moments.

2.2. Experimental Database

[15] We created a database that includes 384 concentration time series, or BTCs, from 98 conservative tracer experiments conducted in 44 streams under different quasi-steady hydrologic conditions (10^{-3} to 10^{3} m^3/s), different experimental conditions (BTCs observed from 10^{1} to 10^{5} m downstream the injection point), and different types of lotic environments (Table 1). We grouped the database by the orders of magnitude of discharge (Table 2) to facilitate the analysis and presentation of the statistical regressions in Figures 1 and 2. All BTCs were zeroed to background concentrations and corrected by discharge changes during the experiments as specified in the references or recorded in experimental notes.

3. Results and Discussion

3.1. Statistical Relationships Derived From Temporal Moment Analysis

[16] Information regarding longitudinal mixing and exchange processes can be found in the normalized central moments (moments about the mean). Figure 1a shows that the variance scales in a nonlinear (non-Fickian) form with the mean travel time. If dispersion processes in streams were Fickian, the regression presented in Figure 1a would have a slope of ~1.0, still preserving a scatter pattern that would be associated with the magnitudes of the dispersion coefficient for each experiment (i.e., different intercepts). Non-Fickian dispersion processes have been widely observed in stream ecosystems [e.g., *Fischer*, 1967; *Nordin and Sabol*, 1974; *Nordin and Troutman*, 1980; *Bencala and Walters*, 1983, and references therein], and in heterogeneous porous media [e.g., *Rao et al*., 1980; *Haggerty and Gorelick*, 1995; *Dentz and Tartakovsky*, 2006]. A non-Fickian behavior is, broadly defined, the result of the presence of multiscale heterogeneities that cannot be integrated into a singular dispersion coefficient [*Neuman and Tartakovsky*, 2009]. To date, several approaches have been proposed to better represent non-Fickian transport, which are largely based on the conceptualization of TS processes and/or the definition of smaller representative elementary volumes, where local homogeneities can be integrated in space and time.

[17] We also correlated m_3 versus m_2 and m_3 versus $f(m_1, m_2)$. Figure 2a suggests that solute transport data have a small range in their coefficient of skewness (CSK, equation (7)). The coefficient of skewness is a measure of asymmetry, i.e., when $\mathrm{CSK}=0$ the data is perfectly symmetrical (no tailing), but it is known that solute transport experiences tailing effects due to surface and hyporheic TS, regardless of the type of stream ecosystem. For the 98 tracer tests (384 BTCs), $\mathrm{CSK}=1.18\pm0.08$ (95% confidence bounds). In Figure 2b, we show that the product $m_1\cdot m_2$ is a quasi-linear estimator of m_3 ($R^2=0.96$). This result, although not representing a predefined statistical descriptor on its own, will be later used to define objective functions for predictive solute transport models (see section 3.3.). Not unexpectedly, based on the results from Figure 1, m_1 is a much weaker predictor of the ratio m_3/m_2 ($R^2=0.66$, results not shown), suggesting that a satisfactory bottom-up estimation of normalized central moments is restricted to one level at most.

$$\mathrm{CSK}=\frac{m_3}{(m_2)^{3/2}};\quad \ln\quad(m_3)=\frac{3}{2}\ln\quad(m_2)+\ln\quad(\mathrm{CSK}) \tag{7}$$

3.2. Observed Scale Invariance in Streams and Solute Transport Models

[18] *Nordin and Sabol* [1974] first reported observations revealing persistent skewness (longitudinally) from Eulerian observations of solute transport time distributions. *Nordin and Troutman* [1980] investigated the performance of the Fickian-type diffusion equation (advection dispersion equation (ADE)), and the inclusion of dead zone processes (i.e., TS model (TSM)) to account for the persistence of skewness, concluding that "... the observed data deviate consistently from the theory in that the skewness of the observed concentration distributions decreases much more slowly than the Fickian theory predicts," and that although the inclusion of dead zones "... yields a theoretical skewness coefficient [CSK] considerably larger than that given by the ordinary Fickian diffusion equation," "... the skewness of the observed concentrations does not appear to be decreasing as rapidly as the theory predicts." The skewness of BTCs also do not begin with values as high as those predicted by the TSM (cf. *Nordin and Troutman*, 1980, Figure 3).

[19] The work by *van Mazijk* [2002] reported that tracer experiments conducted to develop the River Rhine alarm model also showed time distributions with persistent CSK along the extensive reach studied ($100\ \mathrm{km} < L < 1000\ \mathrm{km}$; $Q=1170\mathrm{m}^3/\mathrm{s}$; cf. *van Mazijk*, 2002, Figure 6), i.e., $0.93 \le \mathrm{CSK} \le 1.24$. These observations justified the use of the Chatwin-approximation (Edgeworth series) [*Chatwin*, 1980] to predict solute concentrations in space and time, by fixing $\mathrm{CSK}=1$ for the whole river. Further tracer experiments in the River Rhine ($Q=663\mathrm{m}^3/\mathrm{s}, Q=1820\mathrm{m}^3/\mathrm{s}$) supported the existence of a persistent CSK [*van Mazijk and Veling*, 2005].

Table 1. Conservative Solute Transport Database[a]

Stream	Reach Length (km)	Discharge (m^3/s)	State, Country, (Continent[b])	References
Canal Molinos	0.2	0.2–0.4	Colombia (SA)	As referenced by *González-Pinzón* [2008]
Quebrada Lejía	0.3	0.1–0.5	Colombia (SA)	
Subachoque 1	0.3–0.4	0.2–1.3	Colombia (SA)	*González-Pinzón* [2008] and *Camacho and González-Pinzón* [2008]
Subachoque 2	0.1–0.2	0.3–1.9	Colombia (SA)	
Teusacá 1	0.1–0.2	0.3–0.4	Colombia (SA)	
Teusacá 2	0.3–0.4	0.2–1.4	Colombia (SA)	
Rio Magdalena	36–207	1200–1390	Colombia (SA)	*Torres-Quintero et al*. [2006]
Shaver's Cr.	0.1–0.4	0.2	PA, USA (NA)	Unpublished data
Cherry Cr.	0.7–1.3	0.2	WY, USA (NA)	*Briggs et al*. [2013]
Oak Cr.	0.04–0.3	0.02	OR, USA (NA)	Experiments conducted during the Ph.D. dissertation of the first author.
Fuirosos 1	0.2–0.3	0.01	Spain (EU)	
Fuirosos 2	0.2–0.3	0.01	Spain (EU)	
Antietam Cr.	2.6–67	1.2–12.7	MD, USA (NA)	As referenced by *Nordin and Sabol* [1974, Appendix A].
Monocacy River	7.5–34	12.7–22.1	MD, USA (NA)	
Conococheague Cr.	4.4–34	2.6–30.6	MD, USA (NA)	
Chattahoochee River	10.5–104	108–180	GA, USA (NA)	
Salt Cr.	9.3–52	2.5–4.1	NE, USA (NA)	
Difficult Run	0.6–2	0.9–1.1	VA, USA (NA)	
Bear Cr.	1.1–10.9	10.2–10.5	CO, USA (NA)	
Little Piney Cr.	0.6–7.3	1.4–1.6	MO, USA (NA)	
Bayou Anacoco	11–38	2.0–2.7	LA, USA (NA)	
Comite River	6.8–79	0.8–1.0	LA, USA (NA)	
Bayou Bartholomew	3.2–117	4.1–8.1	LA, USA (NA)	
Amite River	10–148	5.7–8.9	LA, USA (NA)	
Tickfau River	6.4–50	2.0–2.9	LA, USA (NA)	
Tangipahoa River	8.2–94	3.5–18.7	LA, USA (NA)	
Red River	5.7–199	108–249	LA, USA (NA)	
Sabine River	7.9–209	127–433	LA, USA (NA)	
Sabine River	17–121	0.7–9.5	TX, USA (NA)	
Mississippi River	35–294	1495–6824	LA, USA (NA)	
Wind/Bighorn River	9.1–181	55–255	WY, USA (NA)	
Copper Cr.	0.2–8.4	1.0–8.7	VA, USA (NA)	
Clinch River	0.7–6.6	5.7–110	VA, USA (NA)	
Powell River	1.0–7.1	3.9–4.1	TN, USA (NA)	
Coachella Canal	0.3–5.5	25.4–26.9	CA, USA (NA)	
Missouri River	66–227	883–977	IA, USA (NA)	
WS1	0.02–0.3	1 l/s–0.06	OR, USA (NA)	*Gooseff et al*. [2003, 2005]; *Haggerty et al*. [2002], unpublished
WS3	0.04–0.7	1 l/s–0.03	OR, USA (NA)	
Lookout Cr.	0.2–0.4	0.3	OR, USA (NA)	*Gooseff et al*. [2003]
Huey Cr.	0.5–1.0	0.1	AN	*Runkel et al*. [1998]
Swamp Oak Cr.	0.1–0.3	0.1	AUS	*Lamontagne and Cook* [2007]
Clackamas River	9.3	36.8	OR, USA (NA)	*Lee* [1995]
Uvas Cr.	0.04–0.4	0.01	CA, USA (NA)	*Bencala and Walters* [1983]
River Mimram	0.1–0.2	0.3	UK (EU)	*Lees et al*. [2000]

[a]A total of 98 tracer experiments with 384 BTCs were used in this meta-analysis.
[b]SA: South America; NA: North America; EU: Europe; AUS: Australia; AN: Antarctica.

[20] *Schmid* [2002] investigated the conditions under which the TSM could represent the persistence of skewness in solute transport processes. *Schmid* [2002] examined the case of a slug injection into a uniform channel and concluded that a small parametric region (a loop right bounded by $A_s/A < 0.008$; cf. *Schmid* [2002, Figure 1]) could generate a nondecreasing CSK. However, this condition was hypothetical and does not play a major role in practice. Such conditions, if they exist, would be logically inconsistent because tailing effects would be inversely proportional to TS. *Schmid* [2002] also examined a more general scenario with a time-varying concentration distribution as an upstream boundary condition, the division of long reaches into hydraulically uniform subreaches and a routing procedure to link temporal moments at both ends of the subreaches. This analysis suggested that "...the TS model has the potential to explain persistent or growing temporal skewness coefficients, if applied to a sequence of subreaches with respective parameter sets different from each other." However, predicting solute transport meeting these conditions is rather impractical.

[21] If a transport theory is to be capable of scaling and predicting solute transport processes, it will have a

Table 2. Conservative Solute Transport Database Grouped by the Orders of Magnitude of Discharge[a]

Discharge Group Q Gr.	Discharge Order of Magnitude (m^3/s)	Number of Experiments
1	10^{-3}	19
2	10^{-2}	37
3	10^{-1}	68
4	10^{0}	131
5	10^{1}	59
6	10^{2}	53
7	10^{3}	17

[a]The regressions presented in Figures 1 and 2 were labeled as described hereafter.

persistent and statistically constant CSK. Our observations of CSK being statistically constant for widely different hydrodynamic conditions suggest that CSK is not only persistent for a given stream (with distance traveled downstream), but can also be used to scale and predict solute transport processes across ecosystems. At a minimum, a persistent value of CSK is a test that a theory of solute transport must pass.

[22] We used the theoretical temporal moments of three models commonly used for the analysis of in-stream solute transport (ADE, TSM, and the aggregated dead zone model (ADZM)) to calculate their theoretical CSK. If these models were systematically capable of representing the

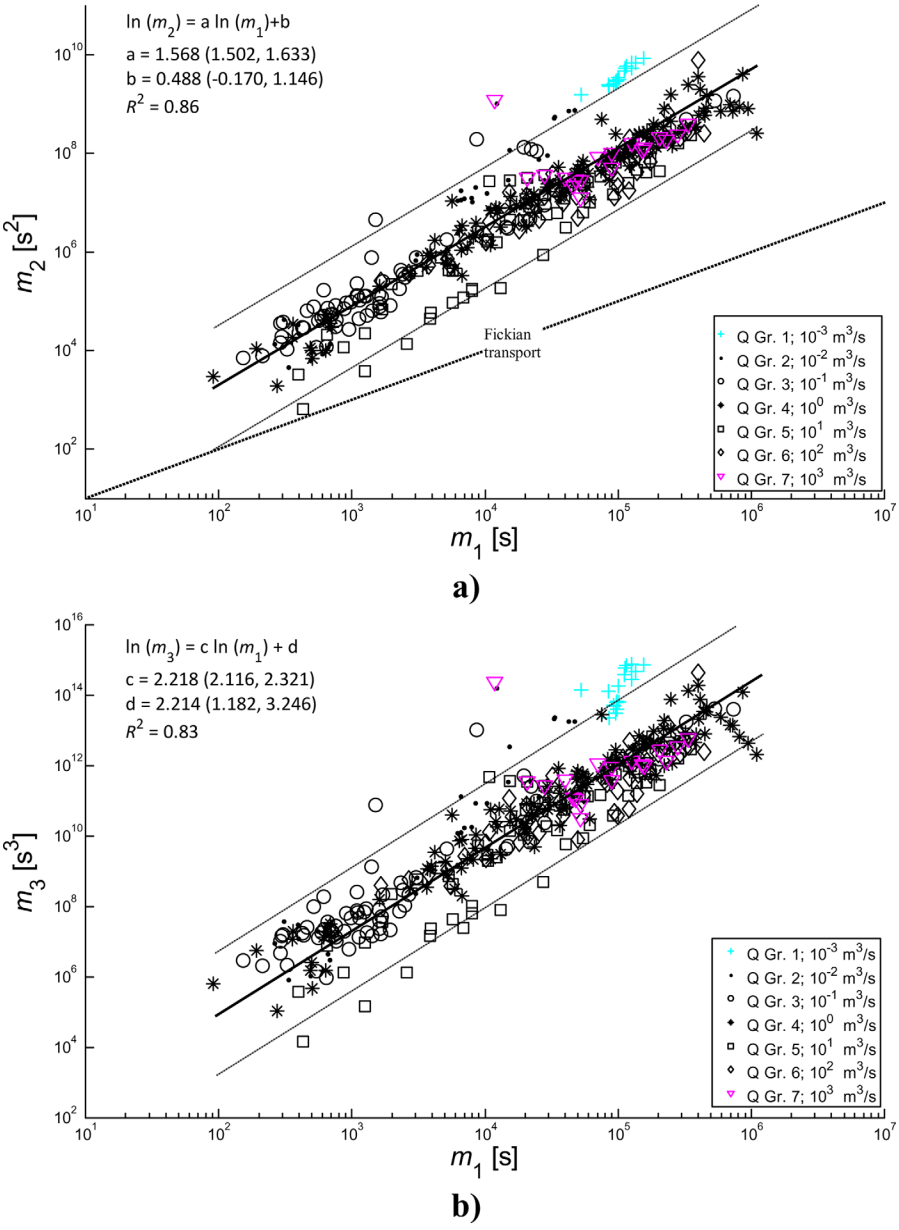

Figure 1. Meta-analysis ($n = 384$ BTCs) of conservative solute transport experiments in streams demonstrates the general occurrence of non-Fickian dispersion processes. (a) The growth rate of the variance is nonlinear (therefore non-Fickian) with respect to the mean travel time; the thick dashed line represents the slope pattern of Fickian dispersion. (b) Skewness as a function of the mean travel time. Coefficients were fitted with 95% confidence bounds. Thin dashed lines represent 95% prediction bounds.

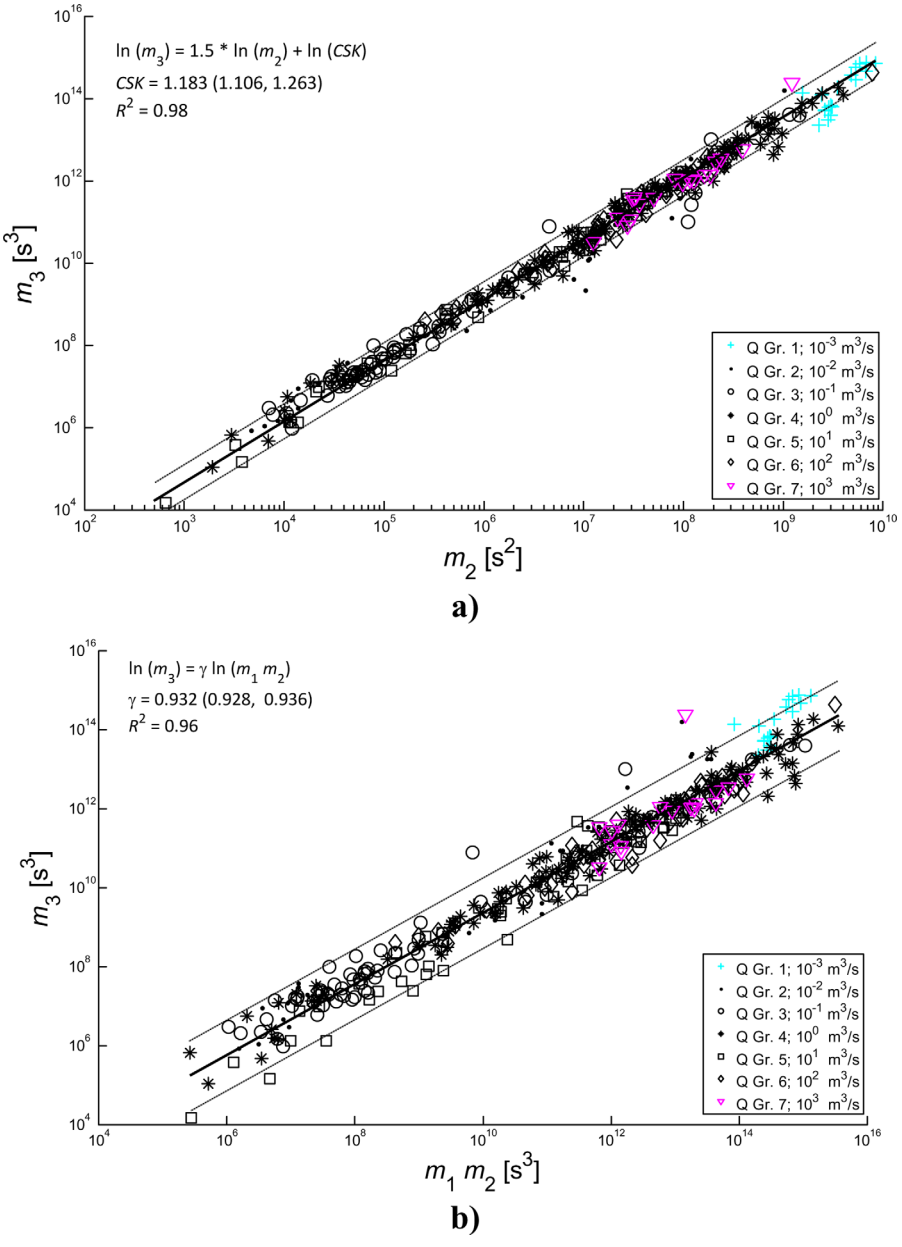

Figure 2. (a) Meta-analysis ($n = 384$ BTCs) of conservative solute transport experiments from contrasting stream ecosystems suggests that the coefficient of skewness holds statistically constant. Fitted coefficients defined CSK $= 1.18 \pm 0.08$. (b) The factor $[m_1 m_2]$ is a quasi-linear estimator of m_3. However, using m_1 to define the ratio $[m_3/m_2]$ yields an $R^2 = 0.66$, showing that a satisfactory bottom-up estimation of normalized central moments is restricted to one level, at most. Coefficients were fitted with 95% confidence bounds. Thin dashed lines represent 95% prediction bounds.

scale-invariant patterns observed in our meta-analysis, the parameters would be self-consistent when describing CSK. The model equations and the theoretical temporal moments and CSKs (calculated for an impulse-type boundary condition, e.g., *Cunningham and Roberts* [1998]) are shown below, along with the consequences of the invariance of CSK on the model parameters. We also included in our analysis (see section 3.2.4) three additional transport models less commonly used to describe solute transport in streams, but that have been used in groundwater systems.

3.2.1. Advection Dispersion Equation

[23]
$$\frac{dC}{dt} = -\frac{Q}{A}\frac{dC}{dx} + D\frac{d^2C}{dx^2} \tag{8}$$

$$\begin{aligned} m_1 &= \tau \\ m_2 &= 2\tau^2/Pe \\ m_3 &= 12\tau^3/Pe^2 \\ \mathrm{CSK}_{\mathrm{ADE}} &= 3\sqrt{2}/\sqrt{Pe} \end{aligned} \tag{9}$$

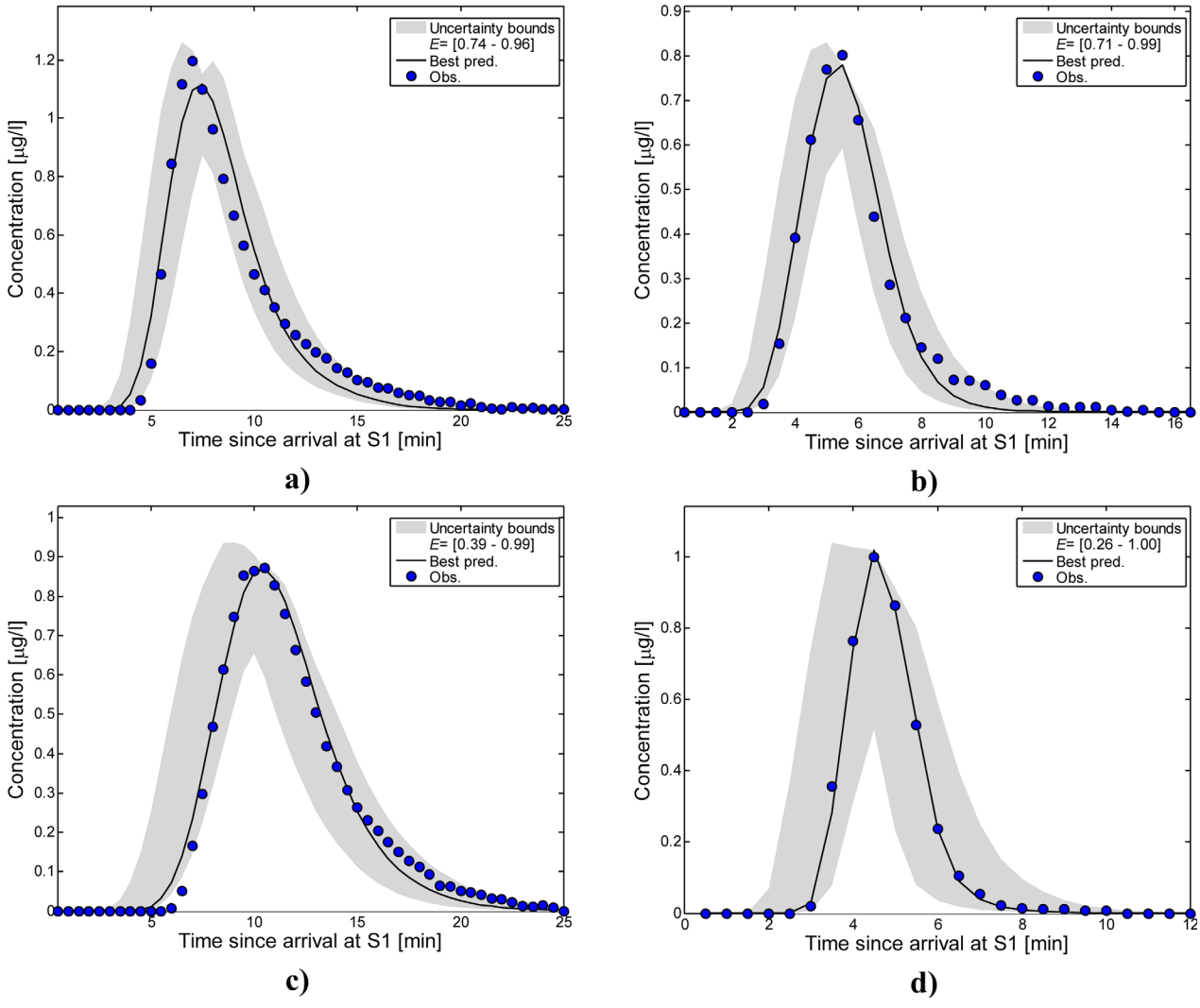

Figure 3. Predicted results using empirical relationships derived from normalized central moment meta-analysis ($n = 384$ BTCs) and the moment-matching technique for the TSM. The known variables were L, Q and $m_{1est.}$, and all others were predicted from 1000 Monte Carlo simulations. The effects of uncertainty in estimating m_1 (i.e., $m_{1est.} = \varphi m_{1obs.}$, with $\varphi = [0.8 - 1.2]$), the parameters of the TSM and the fitting coefficients from our meta-analysis are shown as uncertainty bounds. (a) River Brock, (b) River Conder, (c) River Dunsop, and (d) River Ou Beck. Experimental observations from *Young and Wallis* [1993]. The best parameter sets from the simulations are presented in Table 3. Goodness of fit was estimated with the Nash–Sutcliffe model efficiency coefficient (E).

where C $[ML^{-3}]$ is the concentration of the solute in the main channel; Q $[L^3T^{-1}]$ the discharge; A $[L^2]$ the cross-sectional area of the main channel; D $[LT^{-2}]$ the dispersion coefficient; x $[L]$ the reach length; t $[T]$ time; $\tau = x/u$ $[T]$ is the conservative mean travel time; $Pe = xu/D$ the Peclet number; and $u = Q/A$ the mean velocity in the main channel $[LT^{-1}]$.

Table 3. Best Parameter Sets From 1000 Monte Carlo Simulations Using Empirical Relationships Derived From Normalized Central Moment Meta-Analysis ($n = 384$ BTCs) and the Moment-Matching Technique[a]

				TSM			ADZM	
River	Q (m^3/s)	L (m)	D (m^2/s)	β	$\alpha \times 10^5$ (s^{-1})	E	τ_{ADZ}(s)	E
Brock	4.5×10^{-1}	128	2.33	1.31×10^{-2}	9.77	0.96	218.01	0.98
Conder	1.0	116	2.20	8.12×10^{-3}	8.08	0.99	151.95	0.97
Dunsop	5.4×10^{-1}	130	1.33	1.45×10^{-2}	7.89	0.98	332.55	1.00
Ou Beck	3.5×10^{-2}	127	0.67	4.40×10^{-3}	8.92	1.00	135.95	0.76

[a]Study case of four rivers located in the United Kingdom [*Young and Wallis*, 1993; pp. 160–165]. Goodness of fit was estimated with the Nash–Sutcliffe model efficiency coefficient (E).

[24] Equation (9) suggests that if $\mathrm{CSK}_{\mathrm{ADE}}$ is constant, the Peclet number should also be constant. This implies that, under steady-state flow conditions, the dispersion coefficient must scale linearly with the distance traveled. This violates the assumption of spatially uniform coefficients. Therefore, the ADE with spatially uniform coefficients is incapable of representing the experimental observations. Dispersion coefficients scaling with distance have been widely observed in porous media [e.g., *Pickens and Grisak*, 1981; *Silliman and Simpson*, 1987, *Pachepsky et al*., 2000, and references therein]. Note that the ADE with constant coefficients predicts BTCs with longitudinally decreasing skewness ($\mathrm{CSK}_{\mathrm{ADE}} \sim x^{-1/2}$), becoming asymptotically Gaussian (i.e., $\mathrm{CSK}_{\mathrm{ADE}\,(x\to\infty)} = 0$).

3.2.2. Transient Storage Model

[25]
$$\frac{\partial C}{\partial t} = -\frac{Q}{A}\frac{\partial C}{\partial x} + D\frac{\partial^2 C}{\partial x^2} - \frac{A_s}{A}\alpha_2(C - C_s) \tag{10a}$$

$$\frac{\partial C_s}{\partial t} = \alpha_2(C - C_s) \tag{10b}$$

$$m_1 = \tau(1+\beta)$$

$$m_2 = \frac{2(1+\beta)^2\tau^2}{Pe} + \frac{2\beta\tau}{\alpha_2}$$

$$m_3 = \frac{12(1+\beta)^3\tau^3}{Pe^2} + \frac{12\tau^2\beta(1+\beta)}{\alpha_2 Pe} + \frac{6\beta\tau}{(\alpha_2)^2}$$

$$\mathrm{CSK}_{\mathrm{TSM}} = \frac{3\tau\left(Pe^2\beta + 2\alpha_2\tau Pe\beta(1+\beta) + 2\alpha_2{}^2\tau^2(1+\beta)^3\right)}{\sqrt{2}\alpha_2{}^2 Pe^2\left(\frac{\beta\tau}{\alpha_2} + \frac{(1+\beta)^2\tau^2}{Pe}\right)^{3/2}} \tag{11}$$

where C_s $[ML^{-3}]$ is the concentration of the solute in the storage zone; A_s $[L^2]$ is the cross-sectional area of the storage zone; α_2 $[T^{-1}]$ is the mass-exchange rate coefficient between the main channel and the storage zone; and $\beta = A_s/A$. Other variables are as defined for the ADE. The TSM in equation (10a) is the same presented by *Bencala and Walters* [1983] and *Runkel* [1998] for a reach without lateral inputs, with a slightly different definition of $\alpha_2 = \alpha/\beta$. Note that $\mathrm{CSK}_{\mathrm{TSM}} = \mathrm{CSK}_{\mathrm{ADE}}$ when $\beta = 0$.

[26] If dispersion effects were assumed negligible [e.g., *Wörman*, 2000; *Schmid*, 2002], $\mathrm{CSK}_{\mathrm{TSM}}$ in equation (11) would simplify to

$$\mathrm{CSK}_{\mathrm{TSM}:(D=0)} = \frac{3}{\sqrt{2\alpha_2\beta\tau}} = \frac{3}{\sqrt{2\alpha\tau}} \tag{12}$$

[27] Using the CSK value found in our meta-analysis, the mean residence time in the storage zones ($t_s = 1/\alpha_2$) normalized by β scale linearly with travel time (τ), i.e.,

$$\frac{t_s}{\beta} = \tau\frac{2}{9}(\mathrm{CSK})^2 \Rightarrow \frac{t_s}{\beta} \approx \frac{\tau}{(3.23 \pm 0.4)} \tag{13}$$

[28] Equations (11) and (12) suggest that the standard TSM generates BTCs with longitudinally decreasing skewness ($\mathrm{CSK}_{\mathrm{TSM}} \sim x^{-1/2}$), becoming asymptotically Gaussian (i.e., $\mathrm{CSK}_{\mathrm{TSM}\,(x\to\infty)} = 0$). The physical meaning of the parameters describing $\mathrm{CSK}_{\mathrm{TSM}} = \text{constant}$ is unclear unless dispersion is assumed negligible ($D = 0$). In this case, equation (13) suggests that the TSM model parameters are not independent and that their ratio grows with distance traveled. This analysis supports the results of other studies showing problems of equifinality for the TSM [e.g., *Wagner and Harvey*, 1997; *Wagener et al*., 2002; *Camacho and González-Pinzón*, 2008; C. Kelleher et al., Stream characteristics govern the importance of transient storage processes, submitted to *Water Resources Research*, 2012]. Equations (11) and (13) suggest that the physical meaning of the TSM parameters is limited, and that relationships between TSM parameters and biogeochemical processing may be site dependent (as was discussed in section 1) or even experiment dependent.

3.2.3. Aggregated Dead Zone Model

[29]
$$\frac{\mathrm{d}C}{\mathrm{d}t} = \frac{1}{T_r}[C_u(t - \tau_{\mathrm{ADZ}}) - C(t)] \tag{14}$$

$$\begin{aligned} m_1 &= n(\tau_{\mathrm{ADZ}} + T_r) \\ m_2 &= nT_r{}^2 \\ m_3 &= 2nT_r{}^3 \\ \mathrm{CSK}_{\mathrm{ADZM}} &= 2/\sqrt{n} \end{aligned} \tag{15}$$

where T_r $[T]$ is the lumped ADZ residence time parameter representing the component of the overall reach travel time associated with dispersion; C_u $[ML^{-3}]$ is the known concentration at the input or upstream location; and τ_{ADZ} $[T]$ is the time delay describing solute advection due to bulk flow movement.

[30] Equation (14) describes the mass balance of an imperfectly mixed system (ADZ representative volume), where a solute undergoes pure advection, followed by dispersion in a lumped active mixing volume [*Lees et al*., 2000]. In the ADZM, the distance x implicitly appears in the model description through the time parameters. Note that when $n = 1$, the mean travel time (m_1) could be written as $m_1 = x/u$. In equation (15), the parameter n represents the number of identical ADZ elements serially connected ($n = 1$ for a single ADZ representative volume) to route the upstream boundary condition. The serial ADZM, although capable of representing a persistent CSK, would require the specification of the nonphysical parameter n. More complex ADZM structures can be defined under the database mechanistic approach [e.g., *Young*, 1998], but we restricted our discussion to those that have been more commonly used in stream solute transport modeling [*Young and Wallis*, 1993; *Lees et al*., 2000; *Camacho and González-Pinzón*, 2008; *Romanowicz et al*., 2013].

3.2.4. Alternative Solute Transport Models

[31] Similar sets of calculations also show that the multirate mass transfer (MRMT) model [*Haggerty and Gorelick*, 1995; *Haggerty et al*., 2002] (Appendix A) and a decoupled continuous time random walk (dCTRW) model [e.g., *Dentz and Berkowitz*, 2003; *Dentz et al*., 2004; *Boano et al*., 2007] (Appendix B) are equally incompatible with observations of persistent skewness. The CSK in both of these models also scales as $\mathrm{CSK} \sim x^{-1/2}$.

[32] We also explored a Lévy-flight dynamics model (LFDM) (Appendix C) [e.g., *Shlesingerm et al*., 1982; *Pachepsky et al*., 1997, 2000; *Sokolov*, 2000], which describes the motion of particles behaving similarly to Brownian motion, but allowing occasional clusters of large jumps (significant deviations from the mean). Lévy-flight

models have constant transition times, combined with transition length distributions that are characterized by power-law behaviors for large distances. Therefore, such models represent processes characterized by large velocities for long transitions and low velocities for short transitions, and would account for transport in the continuum of river and storage, with the high velocities present in the stream. We were able to generate an LDFM with persistent CSK for a Lévy distribution parameter $\alpha = 1$ (this α is different from the mass-exchange rate coefficient used in the TSM and MRMT model, (cf. (C2) and (C31)). However, $\alpha = 1$ gives an inconsistent scaling of the variance with distance, i.e., $m_2 \sim x^2$ (cf. (C25)). Furthermore, this distribution parameter would imply a velocity distribution in the stream that scales as $p(u) \sim u^{-2}$ at large velocities, which does not appear realistic.

3.2.5. Remarks on Existent Solute Transport Models

[33] To preserve CSK, the parameters in the solute transport models, including common versions of the CTRW and MRMT, must change with travel distance. Solute transport parameters therefore have some degree of scale dependence (and arbitrariness) imposed by the constant CSK. Furthermore, these parameters have scaling patterns that are unrelated to anything that can currently be measured in the field. These inconsistencies might be because (1) the common solute transport models and assumptions are partly incorrect or (2) we (the stream research community) have collected erroneous observations for decades. The latter condition is possible, but is not likely the explanation for a problem that has been observed across so many data sets. The worst-case scenario in our meta-analysis is that all BTCs were truncated prematurely, due to lack of instrument sensitivity or other reasons. However, this would generate BTCs with larger CSK and would contradict the asymptotic behavior shown for CSK in the transport models discussed above. Consequently, we suspect that our models do not correctly represent one or more aspects of solute transport processes from the field.

3.3. Use of Moments Scaling Properties to Predict Solute Transport

[34] While the models contain an error that needs correction, it may be possible (in the meantime) to adjust the parameters in a way that is predictive of field behavior. In this section, we use the regressions from the temporal moment analysis (section 3.1.) to predict solute transport. We provide the parameterization of the TSM, ADZM, and two probability distributions. We then provide an example using data from tracer experiments that were conducted in the River Brock, River Conder, River Dunsop, and River Ou Beck in the United Kingdom [*Young and Wallis*, 1993, pp. 160–165]. The first three rivers are natural, and River Ou Beck is a concrete urban channel.

[35] The methodology requires an independent estimation of the mean travel time (m_1). One way to do this is to regress m_1 against discharge (Q) using a power law or an inverse relationship in Q [*Young and Wallis*, 1993; *Wallis et al.*, 1989; *Pilgrim*, 1977; *Calkins and Dunne*, 1970]. Once m_1 is estimated, the results from our temporal moment analysis can be used to constrain predictive (forward) simulations of solute transport models. We exemplify this methodology using the experiments by *Young and Wallis* [1993], which were not used in the previous moment analysis, because they show the technique to estimate mean travel times from discharge.

3.3.1. Predicted Solute Transport With Classic Solute Transport Models

[36] The parameters of solute transport models can be determined by matching theoretical and experimental moments. Here, we show how the empirical scaling relationships described in section 3.1 can be used to direct the search of the parameters of the TSM and the ADZM in predictive simulations.

3.3.1.1. Predicted Solute Transport With TSM

[37] We used the empirical relationships derived for m_3 versus m_2 and m_3 versus $f(m_1, m_2)$ (Figure 2) to match the theoretical moment equations presented by *Czernuszenko and Rowinski* [1997]. These theoretical equations have been developed for a general upstream boundary condition with tracer distribution $C(t)$. The parameters for the TSM are those defined by *Bencala and Walters* [1983] and *Runkel* [1998].

$$m_1 = \frac{2D}{u^2} + \frac{L}{u}(1+\beta) \tag{16}$$

$$m_2 = \frac{8D^2}{u^4} + \frac{L}{u}\frac{2D}{u^2}(1+\beta) + \frac{2L}{u}\frac{\beta^2}{\alpha} \tag{17}$$

$$\begin{aligned} m_3 = {} & \frac{2L^2}{u^2}\frac{D}{u^2}(1+\beta)^2\beta + \frac{64D^3}{u^6} \\ & + \frac{L}{u}\left[\frac{12D^2}{u^4}(1+\beta)^2 + \frac{4D}{u^2}\frac{\beta^2}{\alpha}(\beta+2) + \frac{6\beta^3}{\alpha^2}\right] \end{aligned} \tag{18}$$

[38] We have eight variables, i.e., the dispersion coefficient D, β ($\beta = A_s/A$), the mass-transfer rate α, the length of the reach L, the discharge Q ($u = Q/A$), and the normalized central moments m_1, m_2, m_3. We have five equations: three for the theoretical moments (equations (16)–(18)) and two empirical relationships (derived from Figure 2). To balance the degrees of freedom ($n = 8$), we therefore need to specify three ($3 = 8 - 5$) variables, namely L, Q, and m_1. We used a Newton-Raphson algorithm to solve for the five unknowns by minimizing the objective function (OF) shown in equation (19). We estimated the mean travel time as: $m_{1\text{est.}} = \varphi m_{1\text{obs.}}$, with $\varphi = [0.8 - 1.2]$, and randomly varied the regression coefficients of our meta-analysis within the 95% confidence bounds.

$$\begin{aligned} \mathrm{OF}_1 &= \mathrm{abs}\left[1 - \frac{\mathrm{CSK}_{\text{theor.}}}{\mathrm{CSK}_{\text{empirical}}}\right] = \mathrm{abs}\left[1 - \frac{\mathrm{CSK}_{\text{theor.}}}{1.18(\pm 0.08)}\right] \\ \mathrm{OF}_2 &= \mathrm{abs}\left[1 - \frac{\ln[m_{3\text{theor.}}]}{\ln[m_{3\text{empirical}}]}\right] = \mathrm{abs}\left[1 - \frac{\ln[m_{3\text{theor.}}]}{0.932(\pm 0.04)\ln[m_{1\text{est.}} m_2]}\right] \\ \mathrm{OF}_3^* &= \mathrm{abs}\left[1 - \frac{m_{1\text{theor.}}}{m_{1\text{est.}}}\right] \\ \mathrm{OF} &= \mathrm{OF}_1 + \mathrm{OF}_2 + \mathrm{OF}_3^* \end{aligned} \tag{19}$$

[39] In the optimization routine, we allowed the TSM parameters to vary within ranges typically found in similar streams, i.e., $D = [10^{-3}, 10^{1}]$ (m^2/s), $A_s = [10^{-5}, 10^{1}]$ (m^2), $A = [10^{-3}, 10^{1}]$ (m^2), $\alpha = [10^{-7}, 10^{-4}]$ (s^{-1}). Once the system of equations was optimized for each random set

Table 4. List of Estimated Parameters and Prediction Efficiencies for Each Predictive Model Explored[a]

Predictive Model	Estimated Parameters Besides $m_{1est.} = [0.8 - 1.2] \cdot m_{1obs.}$	Prediction Efficiency (E)			
		River Brock	River Conder	River Dunsop	River Ou Beck
TSM	A_s/A, α, D, Q^b, L^b	0.74–0.96	0.71–0.99	0.39–0.99	0.26–1.00
ADZM	τ_{ADZ}	0.50–0.98	0.21–0.97	0.48–1.00	−0.26–0.76
Gumbel dist.	m_2	0.39–0.96	0.45–0.95	0.38–0.99	0.18–0.77
Lognormal dist.	m_2	0.42–0.94	0.47–0.92	0.45–0.97	0.18–0.74

[a]The 1000 Monte Carlo simulations were run per model using empirical relationships derived from normalized central moment meta-analysis ($n = 384$ BTCs). Study case of four rivers located in the United Kingdom [*Young and Wallis*, 1993, pp. 160–165]. $m_{2est.} = (m_{1est.})^{\theta}$, with $\theta = [1.601 - 1.629]$
[b]In the predictive TSM simulations, we entered the actual discharge Q and reach length L.

of estimated mean travel time and fitting coefficients ($n = 1000$), we ran a forward simulation using the optimum parameters. Results from the Monte Carlo simulations are presented in Figure 3 and Tables 3 and 4. We used the Nash–Sutcliffe model efficiency coefficient (E) [*Nash and Sutcliffe*, 1970] to estimate the goodness of fit of the predictions, i.e., how well the plot of observed versus simulated data fits a 1:1 line.

3.3.1.2. Predicted Solute Transport With ADZM

[40] The two parameters of this model are the advection time delay, τ_{ADZ}, and the residence time, $T_r = \overline{t} - \tau_{\mathrm{ADZ}}$, where $\overline{t}$ is the mean travel time (m_1). The theoretical moments of the ADZM for one first-order ADZ element ($n = 1$) were presented in equation (15). Since the mean travel time is a measured or estimated quantity, we only need to solve for the advection time delay, τ_{ADZ}. We applied the same optimization routine described for the TSM, and the results obtained are presented in Figure 4 and Tables 3 and 4.

3.3.2. Predicted Solute Transport With Probability Distributions

[41] Time series described by probability distributions can be used to predict solute transport processes. Here, we show how the empirical scaling relationships described in section 3.1 can be used to estimate the temporal moments of two probability distributions and then to perform predictive simulations.

3.3.2.1. Predicted Solute Transport With Gumbel Distribution

[42] We chose the Gumbel (Extreme Value I) probability distribution because of its constant $\mathrm{CSK}_{\mathrm{Gumbel}} = 1.1395$, which closely agrees with the empirical relationships derived from our meta-analysis ($\mathrm{CSK} = 1.18 \pm 0.08$). This distribution is typically used to describe hydrologic events pertaining to extremes [*Brutsaert*, 2005]. The concentration distribution of a solute BTC using this distribution takes the form:

$$\begin{aligned} C(t) &= m_0 \frac{\exp(-z(t)) \cdot \exp(-\exp(-z(t)))}{\beta} \\ z(t) &= \frac{t - \mu}{\beta} \\ \mu &= m_1 - \beta \cdot 0.5772 \\ \beta &= \sqrt{\frac{6m_2}{\pi^2}} \end{aligned} \tag{20}$$

where μ and β are the location (mode) and scale parameters, respectively. Note that these parameters, and those of any other probability distribution, have no direct physical interpretation.

[43] The use of probability distributions requires the explicit definition of moments beyond the mean travel time, i.e., variance and in some cases the skewness. Therefore, we would need to use empirical relationships such as those derived in Figure 1, even though $R^2 < 0.9$. In our predictive analysis, we used $m_{1\mathrm{est.}} = \varphi m_{1\mathrm{obs.}}$, with $\varphi = [0.8 - 1.2]$ to estimate the uncertainty of $m_{1\mathrm{est.}}$, and $m_{2\mathrm{est.}} = (m_{1\mathrm{est.}})^{\theta}$, with $\theta = [1.601 - 1.629]$, as it was suggested by our meta-analysis (i.e., $\ln m_2 = 1.615(1.601, 1.629) \cdot \ln m_1$, $R^2 = 0.86$, regression not shown in Figure 1). The results obtained are presented in Figure 5 and Table 4.

3.3.2.2. Predicted Solute Transport With Lognormal Distribution

[44] A random variable described by a lognormal distribution comes from the product of n variables, each with its own arbitrary density function with finite mean and variance. This distribution has been widely used in hydrologic modeling of flood volumes and peak discharges, duration curves for daily streamflow, and rainfall intensity-duration data [*Chow*, 1954; *Stendinger*, 1980]. Applications in solute transport suggested that the solute velocity, saturated hydraulic conductivity, and dispersion coefficient are lognormally distributed [*Rogowski*, 1972; *Van De Pol et al.*, 1977; *Russo and Bresler*, 1981]. The concentration distribution of a solute BTC with this distribution takes the form:

$$\begin{aligned} C(t) &= \frac{m_0}{\sigma_n t \sqrt{2\pi}} \exp\left[-\frac{1}{2}\left(\frac{\ln(t) - \mu_n}{\sigma_n}\right)^2\right] \\ m_1 &= \exp\left(\mu_n + \sigma_n^2/2\right) \\ m_2 &= m_1^2\left[\exp\left(\sigma_n^2\right) - 1\right] \end{aligned} \tag{21}$$

where μ_n and σ_n are the mean and the standard deviation of $\ln(t)$. In our predictive analysis, we followed the same procedure described for the Gumbel distribution. The results obtained are presented in Figure 6 and Table 4.

3.3.3. Analysis of Predictive Solute Transport Modeling

[45] In our predictive analyses, we used two classic models (TSM and ADZM) and hypothesized that these models could adequately predict solute transport if the results of our meta-analysis were defined as objective functions to minimize the differences between the theoretical and empirical temporal moments. Our main goal therefore was

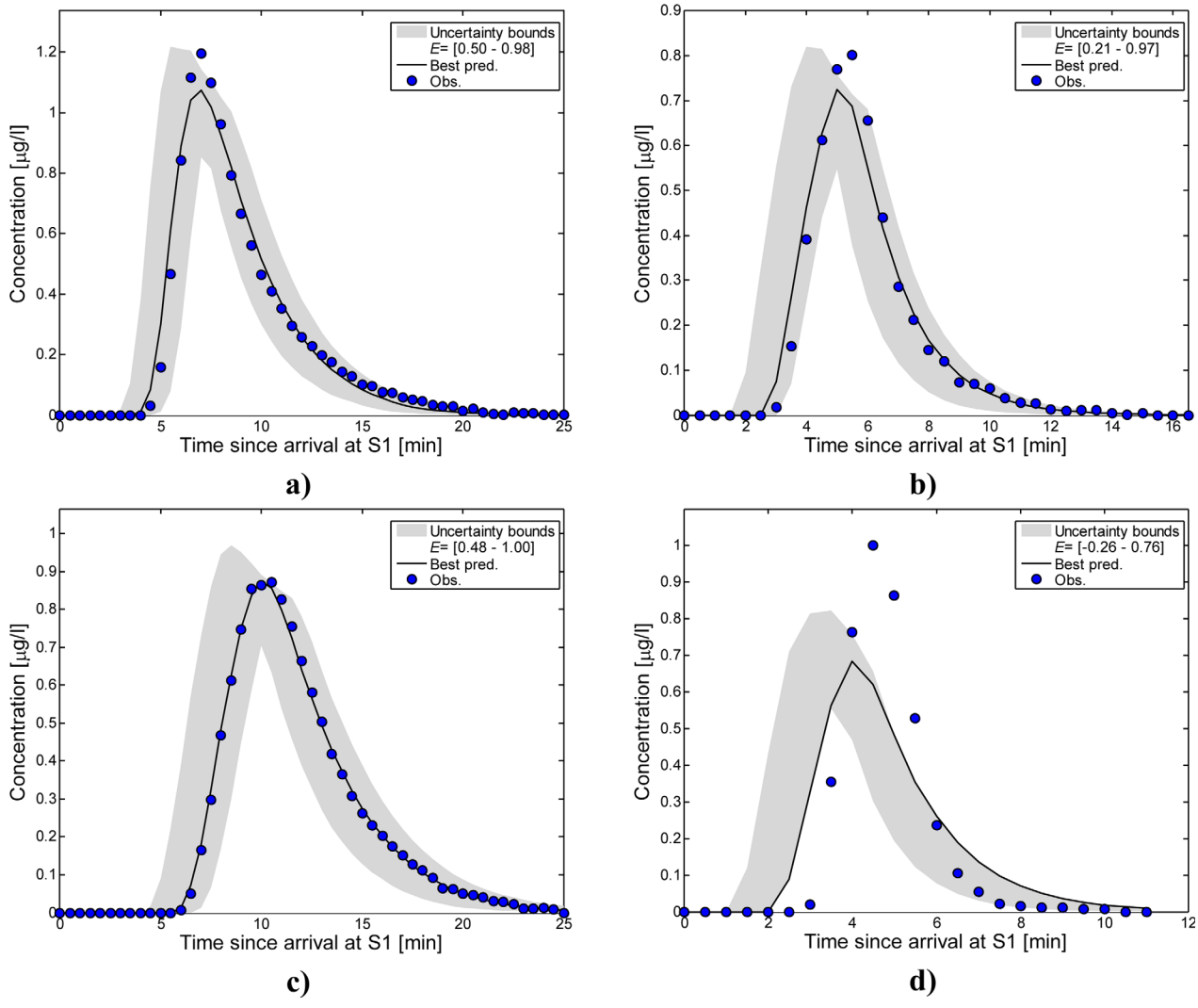

Figure 4. Predicted results using empirical relationships derived from normalized central moment meta-analysis ($n = 384$ BTCs) and the moment-matching technique for the ADZM. The known variable was m_1 (or $\bar{t}$), and τ_{ADZ} was predicted from 1000 Monte Carlo simulations. The effects of uncertainty in m_1 (i.e., $m_{1est.} = \varphi m_{1obs.}$, with $\varphi = [0.8 - 1.2]$) and the fitting coefficients from our meta-analysis are shown as uncertainty bounds. (a) River Brock, (b) River Conder, (c) River Dunsop, and (d) River Ou Beck. Experimental observations from *Young and Wallis* [1993]. The best parameter sets from the simulations are presented in Table 3. Goodness of fit was estimated with the Nash–Sutcliffe model efficiency coefficient (E).

to fix a constant CSK regardless of the longitudinal positioning. The predictive results presented in Figures 3 and 4 and Tables 3 and 4 show that this approach required only basic information (i.e., Q, L, and an estimation of the mean travel time) to adequately predict the behavior of the solute plumes traveling downstream. For the TSM (four parameters), the best predictions in the uncertainty analysis had $E > 0.96$ for the four rivers. For the ADZM (two parameters), the best predictions had $E > 0.97$ for all natural rivers, and $E = 0.76$ for the concrete channel. Although satisfactory results can be achieved with this predictive methodology, it is important to bear in mind that good fittings do not necessarily come from adequate interpretations of mechanistic processes and, therefore, the physical meaning of the parameters should not be taken literally in both inverse (used for calibration) and forward (predictive) simulations.

[46] Besides from predicting solute transport with classic models, we explored the use of probability distributions. We developed predictive models through the parameterization of the Gumbel and lognormal probability distributions, using the results from our meta-analyses and performing uncertainty estimations. The results of our predictive simulations can be summarized as (Table 4): (1) the Gumbel distribution ($CSK_{Gumbel} = 1.1395$) yielded better predictions when the distributions were parameterized with the observed m_1 and m_2, suggesting that $CSK = 1.18 \pm 0.08$ is a consistent pattern derived from our meta-analysis and (2) estimating the variance (m_2) of the distributions from the mean travel time (m_1) can be highly uncertain, and it is explicitly required for using probability distributions in predictive mode; therefore, uncertainty analysis must be always included. Importantly, the parameters of these

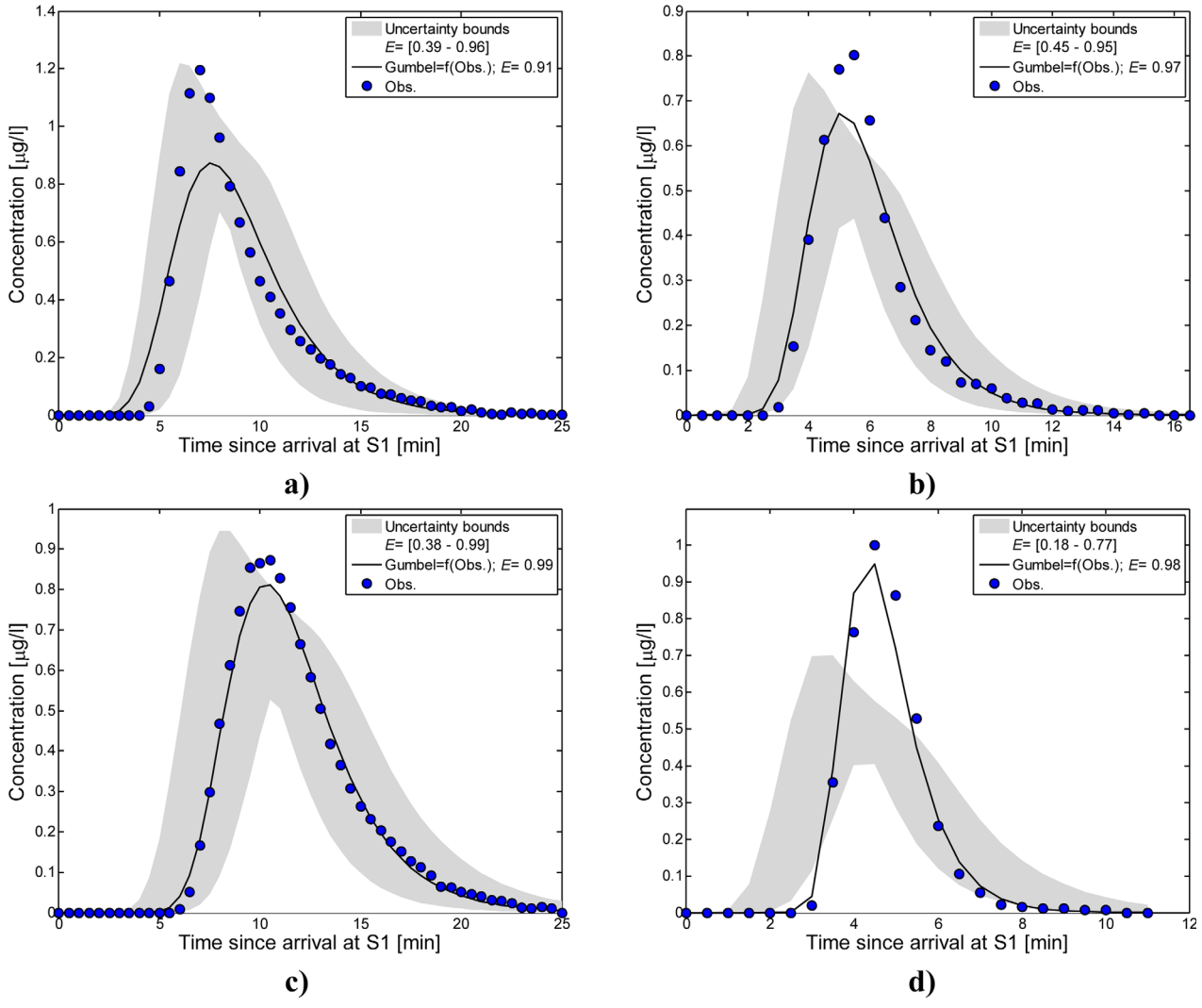

Figure 5. Predicted results using empirical relationships derived from normalized central moment meta-analysis ($n = 384$ BTCs) and the Gumbel distribution, which has a constant $CSK_{Gumbel} = 1.1395$. Uncertainty bounds represent 1000 Monte Carlo simulations where $m_{1est.} = \varphi m_{1obs.}$, with $\varphi = [0.8 - 1.2]$, and $m_{2est.} = (m_{1est.})^{\theta}$, with $\theta = [1.601 - 1.629]$. The "Gumbel=f(Obs.)" simulation uses the actual m_1 and m_2 moments derived from the observed data. (a) River Brock, (b) River Conder, (c) River Dunsop, and (d) River Ou Beck. Experimental observations from *Young and Wallis* [1993]. Goodness of fit was estimated with the Nash–Sutcliffe model efficiency coefficient (E).

distributions do not have direct physical meaning, and this has two main consequences: (1) solute transport understanding cannot be mechanistically advanced and (2) erroneous parametric interpretations from physically based, but poorly constrained models are explicitly avoided.

[47] In summary, we found that the regressions from our meta-analysis can be used to adequately predict solute transport processes using either transport models (fixing CSK) or probability distributions. We consider this a transitional methodology ("a patch solution") between our current understanding and an improved transport theory that better represents the experimental results.

3.4. Implications for Scale-Invariant Patterns

[48] Other experimental findings reveal intriguing similarities to the scale-invariant patterns that we have highlighted here. These include the linear relationship between cross-sectional maximum and mean velocities [*Chiu and Said*, 1995; *Xia*, 1997; *Chiu and Tung*, 2002], and the relatively constant behavior of the dispersive fraction (a parameter derived from the ADZM) in alluvial and headwater streams [*Young and Wallis*, 1993; *González-Pinzón*, 2008]. These observations suggest that stream cross sections establish and tend to maintain a quasi-equilibrium entropic state by adjusting the channel characteristics, i.e., erodible channels adjust their geomorphic characteristics with discharge (bedform and type of sediment transported, slope, alignment, etc.) and nonerodible channels adjust their velocity distributions by changing the maximum velocity and flow depths [*Chiu and Said*, 1995; *Chiu and Tung*, 2002]. An improved solute transport theory should address these observed scale-invariant hydrodynamic patterns and explore the physical meaning of the

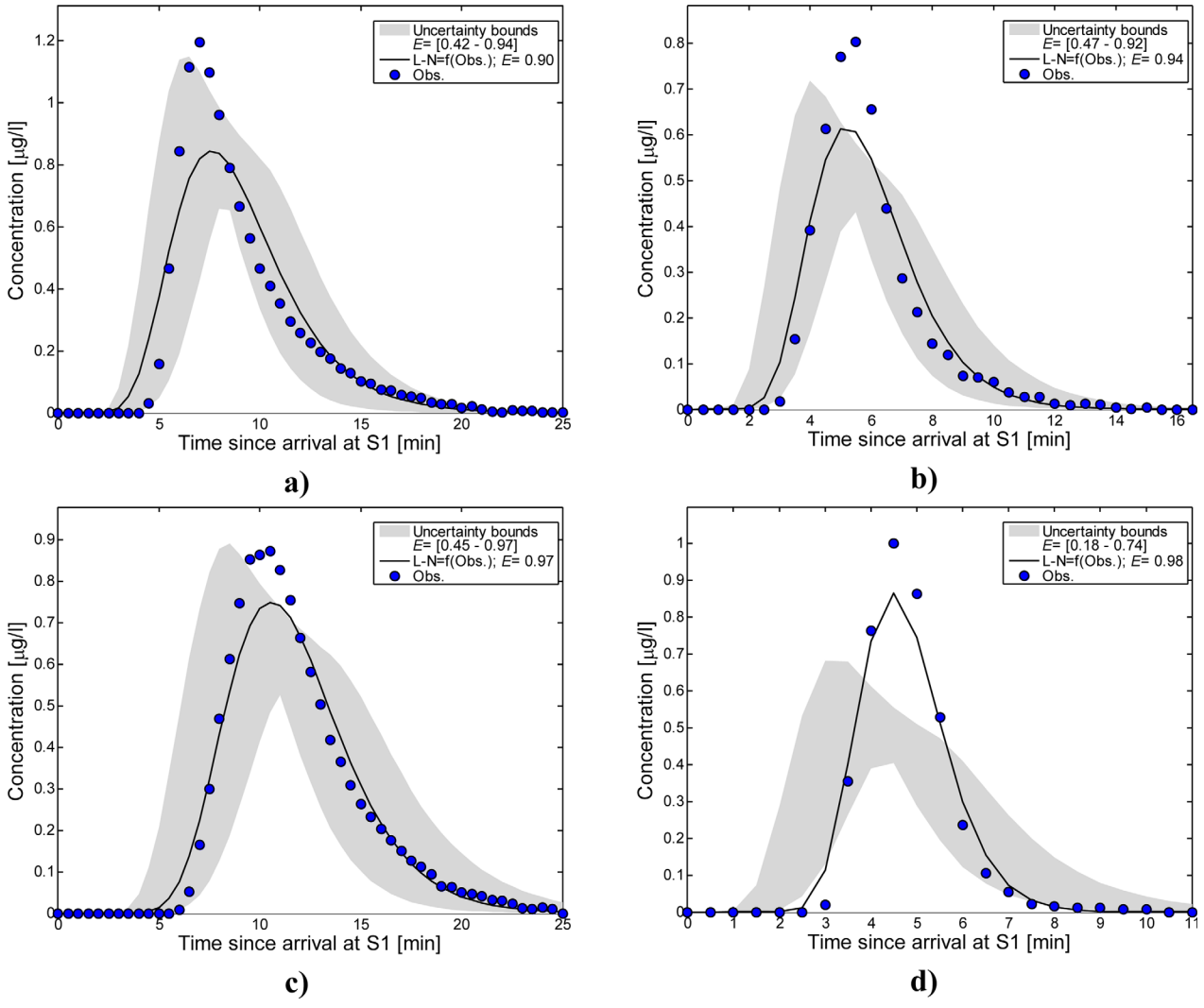

Figure 6. Predicted results using empirical relationships derived from normalized central moment meta-analysis ($n = 384$ BTCs) and the lognormal distribution. Uncertainty bounds represent 1000 Monte Carlo simulations where $m_{1est.} = \varphi m_{1obs.}$, with $\varphi = [0.8 - 1.2]$, and $m_{2est.} = (m_{1est.})^{\theta}$, with $\theta = [1.601 - 1.629]$. The "L-N=f(Obs.)" simulation uses the actual m_1 and m_2 moments derived from the observed data. (a) River Brock, (b) River Conder, (c) River Dunsop, and (d) River Ou Beck. Experimental observations from *Young and Wallis* [1993]. Goodness of fit was estimated with the Nash–Sutcliffe model efficiency coefficient (E).

persistence of skewness, which perhaps could be based on principles of thermodynamics and fluid dynamics.

[49] The coefficient of skewness of the classic solute transport models discussed in section 3.2 shows that Fickian dispersion is inconsistent with the experimental results. The inclusion of macroscopic Fickian dispersion generates a system where the variance of a dispersing solute grows linearly with the distance traveled, generating skewed distributions that later become asymptotically Gaussian [*Fisher et al.*, 1979; *Nordin and Troutman*, 1980]. This behavior is independent of the assumption of hydraulically uniform stream reaches, suggesting that a revised dispersion approach would be needed unless other mechanisms included in the transport theory (e.g., TS) were capable of counteracting the ever decreasing skewness represented by Fickian dispersion.

[50] Although we have not yet investigated scale-invariant behaviors of temporal distributions in processes other than solute transport, we predict that similar patterns can be derived from meta-analysis of flow routing BTCs. We ground this prediction in the fact that the conservative tracers used in our analyses have marked up how water flowed through the different stream ecosystems considered, experiencing similar physical characteristics and processes involved in flow routing (i.e., shear effects, heterogeneity and anisotropy, and dual-domain mass transfer). Regardless of the adequacy of current transport and flow routing modeling approaches, clear similarities appear when comparing the BTCs of these hydrologic processes, and the temporal moments of (for example) the ADZM and those of the Nash cascade [*Nash*, 1960] and the Linear (and Multilinear) Discrete (Lag) Cascade channel routing models

[*O'Connor*, 1976; *Perumal*, 1994; *Camacho and Lees*, 1999]. If similar patterns were found with respect to the persistence of skewness in solute transport and flow routing, this could be advantageously used to better understand, scale, and predict solute transport processes under flow dynamic conditions, which is a problem that still remains largely unresolved [*Runkel and Restrepo*, 1993; *Graf*, 1995; *Zhang and Aral*, 2004].

4. Conclusions

[51] Despite numerous detailed studies of in-stream transport processes [e.g., *Bencala and Walters*, 1983; *Harvey and Bencala*, 1993; *Elliott and Brooks*, 1997a, 1997b; *Gooseff et al*., 2005; *Wondzell*, 2006; *Cardenas et al*., 2008], scaling and predicting solute transport can be highly uncertain. This is primarily due to the difficulties of measuring and incorporating stream hydrodynamic and geomorphic characteristics into models. A consequence of these simplifications is that parameters cannot be obtained uniquely from physical attributes. The parameters are functions of a combination of several processes and physical attributes. Therefore, model parameters interact with each other, and the overall model response to different parameter sets might be numerically "equal" and mechanistically misleading.

[52] Our (model-free) meta-analysis of the BTCs from conservative tracer experiments conducted in a wide range of locations and hydrodynamic conditions suggests that the coefficient of skewness (CSK) is scale invariant and equal to approximately 1.18. Considering the limited information that is currently available on solute transport processes in different catchments around the world, this methodology is perhaps the least biased (different personnel and instrumentation were used to collect the data) and most informative (BTCs sampled a wide range of multiscale heterogeneities) to investigate scaling patterns in stream ecosystems. The self-consistent relationships derived from our extensive database for normalized central temporal moments can be used to adequately predict solute transport. Such relationships also revealed systematic limitations of the solute transport models currently used in hydrology and suggest that we need a revised solute transport theory that is capable of representing the observed scaling patterns.

[53] Because solute transport is the foundation of biogeochemical models, if transport models with unidentifiable parameters are used to investigate the coupling between TS and biochemical reactions across ecosystems, it is not unexpected that the relationships derived are inconclusive, as it has been extensively shown to date. Ultimately, model structural errors generate equifinal systems that can lead to biased conclusions with respect to the nature of mechanistic relationships.

Appendix A: MRMT Model

$$\frac{\partial C}{\partial t}+\beta\int_0^\infty \frac{\partial C_s(\alpha_2)}{\partial t}p(\alpha_2)d\alpha_2=-\frac{Q}{A}\frac{\partial C}{\partial x}+D\frac{\partial^2 C}{\partial x^2} \tag{A1}$$

$$\frac{\partial C_s(\alpha_2)}{\partial t}=\alpha_2(C-C_s(\alpha_2)),0<\alpha_2<\infty \tag{A2}$$

[54] The theoretical temporal moments were computed in a manner similar to *Cunningham and Roberts* [1998]:

$$m_1=\tau(1+\beta)$$

$$m_2=\frac{2\tau^2(1+\beta)^2}{Pe}+2\tau\beta\hat{\mu}$$

$$m_3=\frac{12\tau^3(1+\beta)^3}{Pe^2}+\frac{12\tau^2\beta(1+\beta)}{Pe^2}\hat{\mu}+6\tau\beta\left(\hat{\mu}^2+\hat{\sigma}^2\right)$$

$$\mathrm{CSK}_{\mathrm{MRMT}}=\frac{3\tau\left(2\frac{(1+\beta)^3\tau^2}{Pe^2}+\beta\left(\frac{2(1+\beta)\hat{\mu}\tau}{Pe}+\left(\hat{\mu}^2+\hat{\sigma}^2\right)\right)\right)}{\sqrt{2}\left(\frac{\tau\left((1+\beta)^2\tau+Pe\beta\hat{\mu}\right)}{Pe}\right)^{3/2}} \tag{A3}$$

where $C_s(\alpha_2)$ [ML^{-3}] is the concentration of the solute in the storage zone; p is the probability density function of mass transfer exchange rates; and $\hat{\mu}$ and $\hat{\sigma}^2$ are the mean and variance of the distribution of TS residence times [cf., *Haggerty and Gorelick*, 1995; *Cunningham and Roberts*, 1998]. Other variables are as defined for the TSM. When $\beta=0$, $\mathrm{CSK}_{\mathrm{MRMT}}=\mathrm{CSK}_{\mathrm{ADE}}$. If dispersion is negligible ($D=0$):

$$\mathrm{CSK}_{\mathrm{MRMT:}\,(D=0)}=\frac{3\tau\beta\left(\hat{\mu}^2+\hat{\sigma}^2\right)}{\sqrt{2}(\beta\hat{\mu}\tau)^{3/2}} \tag{A4}$$

[55] If $\mathrm{CSK}_{\mathrm{MRTM}}$ is not fixed, the MRMT model will represent BTCs with longitudinally decreasing skewness ($\mathrm{CSK}_{\mathrm{MRMT}}\sim x^{-1/2}$), becoming asymptotically Gaussian (i.e., $\mathrm{CSK}_{\mathrm{MRMT}\,(x\to\infty)}=0$).

Appendix B: The dCTRW Model

[56] The Laplace transform (LT) of $f(x,t)$ for a dCTRW model is given by *Dentz et al*. [2004]:

$$\overline{f}(x,s)=\exp\left[-\frac{xu}{2D}\left(\sqrt{1+\frac{4M(s)D}{u^2}}-1\right)\right] \tag{B1}$$

where s is the LT variable. Other variables have been defined previously in the ADE. The memory function $M(s)$ is defined by

$$M(s)=\frac{1-\overline{\phi}(s)}{\tau_1\overline{\phi}(s)} \tag{B2}$$

where $\overline{\phi}(s)\equiv\sum\overline{\phi}(x,s)$ is the LT of the time transition probability density function; $\overline{\phi}(x,s)=p(x)\overline{\phi}(s)$ is the LT of a joint space ($p(x)$) and time transition probability density function; and τ_1 is a median transition time. We estimated the temporal moments using the method by *Aris* [1958].

$$
\begin{aligned}
m_1 &= \frac{x}{u}\frac{M(s)'}{\sqrt{1+\frac{4M(s)D}{u^2}}}\Bigg|_{s=0} \\
m_2 &= -\frac{x}{u}\frac{M(s)''}{\sqrt{1+\frac{4M(s)D}{u^2}}} + \frac{2xD}{u^3}\frac{\left(M(s)'\right)^2}{\left(1+\frac{4M(s)D}{u^2}\right)^{3/2}}\Bigg|_{s=0} \\
m_3 &= \frac{x}{u}\frac{M(s)'''}{\sqrt{1+\frac{4M(s)D}{u^2}}} - \frac{4xD}{u^3}\frac{M(s)'\left(M(s)'\right)^2}{\left(1+\frac{4M(s)D}{u^2}\right)^{3/2}} \\
&\quad + \frac{12xD^2}{u^5}\frac{\left(M(s)'\right)^3}{\left(1+\frac{4M(s)D}{u^2}\right)^{5/2}}\Bigg|_{s=0}
\end{aligned}
\tag{B3}
$$

[57] The solution for the Fickian case is found when $M(s) = s$, which yields $\mathrm{CSK}_{\mathrm{Fickian}} = 3\sqrt{2}/\sqrt{Pe}$, as it was shown for the ADE (section 3.2.1). A general pattern for the $\mathrm{CSK}_{\mathrm{dCTRW}}$ can be inferred from this particular condition, and the specifics will depend on the memory function defined for the model. In summary, if $\mathrm{CSK}_{\mathrm{dCTRW}}$ is not fixed, a dCTRW model will represent BTCs with longitudinally decreasing skewness ($\mathrm{CSK}_{\mathrm{dCTRW}} \sim x^{-1/2}$), becoming asymptotically Gaussian (i.e., $\mathrm{CSK}_{\mathrm{dCTRW}\,(x\to\infty)} = 0$).

Appendix C: Lévy-Flight Dynamics Model

[58] We consider here a Lévy-flight type dynamics model, which has a fractal dependence on the sampling position and takes the form:

$$
\begin{aligned}
x_{n+1} &= x_n + \xi_n \\
t_{n+1} &= t_n + \tau_0
\end{aligned}
\tag{C1}
$$

where τ_0 is a constant time increment, and $\xi_n > 0$ are independent identically power law distributed random variables such that:

$$
p(x) \propto x^{-1-\alpha} \tag{C2}
$$

[59] For large α (Lévy-flight variable), $p(x)$ could be a Pareto distribution, for example. The spatial Laplace transform of $p(x)$ for $1 < \alpha < 2$ then would be

$$
\overline{p}(\kappa) = 1 - a\kappa + b\kappa^{\alpha} \tag{C3}
$$

[60] We are interested in the distribution of arrival times $t(x)$ at a position x, which is given by

$$
t(x) = t_{n_x} \tag{C4}
$$

where $n_x = \max(n | x_n < x)$ is the number of steps needed to arrive at position x by the Lévy process shown in equation (C1). It is equivalent to $x_n < x < x_{n+1}$. Thus, we obtain for the arrival time density:

$$
f(x,t) = \langle \delta(t - t_{n_x}) \rangle \tag{C5}
$$

where $\delta(t)$ denotes the Dirac delta distribution and the angular brackets denote the noise average over ξ_n. Expression (C5) can be written as

$$
f(x,t) = \sum_{n=0}^{\infty} \delta(t - t_n) \langle \delta_{n,n_x} \rangle = \sum_{n=0}^{\infty} \delta(t - t_{n_x}) \langle I(0 \le x - x_n \le \xi_n) \rangle \tag{C6}
$$

where $I(0 \le x < \xi)$ is an indicator function that is 1 if the condition in its argument is true and 0 otherwise. The latter equation can be further developed as

$$
f(x,t) = \int_0^x \sum_{n=0}^{\infty} \delta(t - t_{n_x}) \langle \delta(x' - x_n) \rangle \langle I(0 \le x - x' \le \xi_n) \rangle \mathrm{d}x' \tag{C7}
$$

[61] Computing the second average we get:

$$
f(x,t) = \int_0^x R(x',t)\mathrm{d}x' \int_{x-x'}^{\infty} p(\xi)\,\mathrm{d}\xi \tag{C8}
$$

$$
R(x',t) = \sum_{n=0}^{\infty} \delta(t - t_n) \langle \delta(x' - x_n) \rangle \tag{C9}
$$

[62] The latter satisfies the Kolmogorov type equation:

$$
R(x,t) = \delta(x)\delta(t) + \int_0^{\infty} p(\xi) R(x - \xi, t - \tau_0)\mathrm{d}\xi \tag{C10}
$$

[63] Combining equations (C8) and (C10) in Laplace space, we get

$$
\kappa \overline{f}(\kappa,t) = \delta(t) + \overline{M}(\kappa)\left[\overline{f}(\kappa, t - \tau_0) - \overline{f}(\kappa,t)\right] \tag{C11}
$$

$$
\overline{M}(\kappa) = \frac{\kappa \overline{p}(\kappa)}{1 - \overline{p}(\kappa)} \tag{C12}
$$

[64] The time increment τ_0 is supposed to be small compared to the observation time, so that we can write (C11) as

$$
\kappa \overline{f}(\kappa,t) = \delta(t) - \overline{M}(\kappa)\tau_0 \frac{\partial \overline{f}(\kappa,t)}{\partial t} \tag{C13}
$$

[65] In real space, it reads as

$$
\frac{\partial f(x,t)}{\partial t} = -\int_0^x M(\xi)\tau_0 \frac{\partial f(x - \xi, t)}{\partial t}\mathrm{d}\xi \tag{C14}
$$

[66] Defining the moments of $f(x,t)$ by

$$
\mu_n(x) = \int_0^{\infty} t^n f(x,t)\mathrm{d}t \tag{C15}
$$

[67] We obtain from equation (C14) the moment equations

$$
\frac{\partial \mu_n(x)}{\partial x} = n\int_0^x M(\xi)\tau_0 \mu_{i-1}(x - \xi)\mathrm{d}\xi \tag{C16}
$$

where $\mu_n(x) = 0$ for $n < 0$. This equation can, again, be solved in Laplace space:

$$
\kappa \overline{\mu}_n(\kappa) = \delta_{n0}(t) + n\overline{M}(\kappa)\tau_0 \overline{\mu}_{n-1}(\kappa) \tag{C17}
$$

[68] For $n = 1$ we obtain:

$$
\overline{\mu}_1(\kappa) = \overline{M}(\kappa)\kappa^{-2} \tag{C18}
$$

because $\overline{\mu}_0(\kappa) = \kappa^{-1}$. We are interested in the behavior at large distances, which means at small κ. Inserting equation (C12) above gives

$$\overline{\mu}_1(\kappa) = \tau_0 \kappa^{-1} \frac{\overline{p}(\kappa)}{1 - \overline{p}(\kappa)} \tag{C19}$$

[69] Inserting now equation (C3) and expanding up to leading order gives

$$\overline{\mu}_1(\kappa) = \tau_0 \kappa^{-1} \frac{1}{a\kappa - b\kappa^{\alpha}} = \frac{\tau_0}{a^2}\kappa^2 + ... \tag{C20}$$

[70] Thus, the first moment is given by

$$\mu_1(x) = \frac{x\tau_0}{a} \tag{C21}$$

[71] For the second moment, we have

$$\overline{\mu}_2(\kappa) = 2\tau_0^2 \kappa^{-1} \frac{\overline{p}(\kappa)^2}{\left[1 - \overline{p}(\kappa)\right]^2} \tag{C22}$$

[72] Inserting equation (C3) and expanding up to leading orders we have

$$\overline{\mu}_2(\kappa) = 2\frac{\tau_0^2}{a^2\kappa^3} + 4\frac{\tau_0^2 b}{a^3}\kappa^{\alpha-4} + ... \tag{C23}$$

[73] Inversion of this expression gives

$$\mu_2(x) = \frac{\tau_0^2}{a^2}x^2 + 4\frac{\tau_0^2 b}{a^3\Gamma(4-\alpha)}x^{3-\alpha} \tag{C24}$$

[74] The second normalized central moment is

$$m_2(x) = 4\frac{\tau_0^2 b}{a^3\Gamma(4-\alpha)}x^{3-\alpha} \tag{C25}$$

[75] For the third moment, we have

$$\overline{\mu}_3(\kappa) = 6\tau_0^3 \kappa^{-1} \frac{\overline{p}(\kappa)^3}{\left[1 - \overline{p}(\kappa)\right]^3} \tag{C26}$$

[76] Inserting equation (C3) and expanding up to leading orders, we have

$$\overline{\mu}_3(\kappa) = 6\frac{\tau_0^3}{a^3\kappa^4} + 18\frac{\tau_0^3 b}{a^4}\kappa^{\alpha-5} + ... \tag{C27}$$

[77] Inversion of this expression gives:

$$\mu_3(x) = \frac{\tau_0^3}{a^3}x^3 + \frac{18\tau_0^3 b}{a^4\Gamma(5-\alpha)}x^{4-\alpha} \tag{C28}$$

[78] The third normalized central moment is

$$m_3(x) = \frac{3\tau_0^3 b}{a^4}\left[\frac{6}{\Gamma(5-\alpha) - \frac{4}{\Gamma(4-\alpha)}}\right]x^{4-\alpha} \tag{C29}$$

[79] We can now estimate the scaling of CSK as

$$\mathrm{CSK}_{\mathrm{LFDM}} = \frac{m_3(x)}{m_2(x)^{1.5}} \sim \frac{x^{4-\alpha}}{x^{3\cdot(1.5)-\alpha\cdot(1.5)}} \tag{C30}$$

[80] For $\mathrm{CSK}_{\mathrm{LFDM}}$ to be independent of x (or persistent) we need:

$$\alpha = \frac{4 - 3\cdot(1.5)}{1 - 1.5} = 1 \tag{C31}$$

[81] **Acknowledgments.** This work was funded by NSF grant EAR 08–38338. Funding was also available from the HJ Andrews Experimental Forest research program, funded by the National Science Foundation's Long-Term Ecological Research Program (DEB 08–23380), U.S. Forest Service Pacific Northwest Research Station, and Oregon State University. We thank the Associate Editor, Olaf Cirpka, Adam Wlostowski, and an anonymous reviewer for providing insightful comments that helped to improve this manuscript.

References

Argerich, A., R. Haggerty, E. Martí, F. Sabater, and J. Zarnetske (2011), Quantification of metabolically active transient storage (MATS) in two reaches with contrasting transient storage and ecosystem respiration, *J. Geophys. Res.*, *116*, G03034, doi:10.1029/2010JG001379.

Aris, R. (1958), On the dispersion of linear kinetic waves, *Proc. R. Soc. London Ser. A*, *245*, 268–277.

Beer, T., and P. Young (1983), Longitudinal dispersion in natural streams, *J. Environ. Eng.*, *109*(5), 1049–1067.

Bencala, K. E., and R. A. Walters (1983), Simulation of solute transport in a mountain pool-and-riffle stream: A transient storage model, *Water Resour. Res.*, *19*(3), 718–724, doi:10.1029/WR019i003p00718.

Beven, K. (1993), Models of channel networks: Theory and predictive uncertainty, in *Channel Network Hydrology*, edited by K. Beven and M. J. Kirby, pp. 129–173, John Wiley, Chichester, England.

Beven, K. J., and A. M. Binley (1992), The future of distributed models: Model calibration and uncertainty prediction, *Hydrol. Processes*, *6*, 279–298.

Boano, F., A. I. Packman, A. Cortis, R. Revelli, and L. Ridolfi (2007), A continuous time random walk approach to the stream transport of solutes, *Water Resour. Res.*, *43*, W10425, doi:10.1029/2007WR006062.

Botter, G., N. B. Basu, S. Zanardo, P. S. C. Rao, and A. Rinaldo (2010), Stochastic modeling of nutrient losses in streams: Interactions of climatic, hydrologic, and biogeochemical controls, *Water Resour. Res.*, *46*, W08509, doi:10.1029/2009WR008758.

Bukaveckas, P. A. (2007), Effects of channel restoration on water velocity, transient storage, and nutrient uptake in a channelized stream, *Environ, Sci. Technol.*, *41*, 1570–1576.

Briggs, M. A., Lautz, L. K., Hare, D. K., and R. González-Pinzón (2013), Relating hyporheic fluxes, residence times and redox-sensitive biogeochemical processes upstream of beaver dams, *Freshwater Sci.*, *32*, 622–641.

Brutsaert, W. (2005), *Hydrology: An Introduction*, Cambridge Univ. Press, U. K.

Calkins, D., and T. Dunne (1970), A salt tracing method for measuring channel velocities in small mountain streams, *J. Hydrol.*, *11*(4), 379–392.

Camacho, L. A., and R. González-Pinzón (2008), Calibration and prediction ability analysis of longitudinal solute transport models in mountain streams, *J. Environ Fluid Mech.*, *8*(5), 597–604.

Camacho, L. A., and M. J. Lees (1999), Multilinear discrete lag-cascade model for channel routing, *J. Hydrol.*, *226*, 30–47.

Cardenas, M. B., J. L. Wilson, and R. Haggerty (2008), Residence time of bedform-driven hyporheic exchange, *Adv. Water Resour.*, *31*(10), 1382–1386.

Chatwin, P. (1980), Presentation of longitudinal dispersion data, *J. Hydraul. Div.*, *106*(1), 71–83.

Chiu, C.-L., and A. A. Said (1995), Maximum and mean velocities and entropy in open-channel flow, *J. Hydraul. Eng.*, *121*(1), 26–35.

Chiu, C.-L., and N.-C. Tung (2002), Maximum velocity and regularities in open channel flow, *J. Hydraul. Eng.*, *128*(4), 390–398.

Chow, V. T. (1954), The log-probablity law and its engineering applications, *Proc. Am. Soc. Civ. Eng.*, *80*(5), 536-1–536-25.

Cunningham, J. A., and P. V. Roberts (1998), Use of temporal moments to investigate the effects of nonuniform grain-size distribution on the transport of sorbing solutes, *Water Resour. Res.*, *34*(6), 1415–1425, doi:10.1029/98WR00702.

Cvetkovic, V., C. Carstens, J.-O. Selroos, and G. Destouni (2012), Water and solute transport along hydrological pathways, *Water Resour. Res.*, *48*, W06537, doi:10.1029/2011WR011367.

Czernuszenko, W., and P. M. Rowinski (1997), Properties of the dead-zone model of longitudinal dispersion in rivers, *J. Hydraul. Res.*, *35*(4), 491–504.

Das, B. S., R. S. Govindaraju, G. J. Kluitenberg, A. J. Valocchi, and J. M. Wraith (2002), Theory and applications of time moment analysis to study the fate of reactive solutes in soil, in *Stochastic Methods in Subsurface Contaminant Hydrology*, edited by R. S. Govindaraju, pp. 239–279, ASCE Press.

Dentz, M., and B. Berkowitz (2003), Transport behavior of a passive solute in continuous time random walks and multirate mass transfer, *Water Resour. Res.*, *39*(5), 1111, doi:10.1029/2001WR001163.

Dentz, M., and D. Tartakovsky (2006), Delay mechanisms of non-Fickian transport in heterogeneous media, *Geophys. Res. Lett.*, *33*, L16406, doi:10.1029/2006GL027054.

Dentz, M., A, Cortis, H. Scher, and B. Berkowitz (2004), Time behavior of solute transport in heterogeneous media: Transition from anomalous to normal transport, *Adv. Water Resour.*, *27*, 155–173.

Elliott, A. H., and N. H. Brooks (1997a), Transfer of nonsorbing solutes to a streambed with bedforms: Theory, *Water Resour. Res.*, *33*, 123–136.

Elliott, A. H., and N. H. Brooks (1997b), Transfer of nonsorbing solutes to a streambed with bedforms: Laboratory experiments, *Water Resour. Res.*, *33*, 137–151.

Ensign, S. H., and M. W. Doyle (2005), In-channel transient storage and associated nutrient retention: Evidence from experimental manipulations, *Limnol. Oceanogr.*, *50*(6), 1740–1751.

Fischer, H. B. (1967), The mechanics of dispersion in natural streams, *J. Hydraul. Div. Am. Soc. Civ. Eng.*, *93*(HY6), 187–216.

Fisher, H. B., E. J. List, R. C. Koh, J. Imberger, and N. H. Brooks (1979), *Mixing in Inland and Coastal Waters*, Academic, New York.

Goltz, M. N., and P. V. Roberts (1987), Using the method of moments to analyze three-dimensional diffusion-limited solute transport from temporal and spatial perspectives, *Water Resour. Res.*, *23*(8), 1575–1585, doi:10.1029/WR023i008p01575.

González-Pinzón, R. A. (2008), *Determinación del comportamiento de la fracción dispersiva en ríos característicos de montaña*, M.Sc. thesis, Dep. de Ingeniertía Civ. y Agrícola, Univ. Nacl. de Colombia, Bogotá.

Gooseff, M. N., S. M. Wondzell, R. Haggerty, and J. Anderson (2003), Comparing transient storage modeling and residence time distribution (RTD) analysis in geomorphically varied reaches in the Lookout Creek basin, Oregon, USA, *Adv. Water Resour.*, *26*, 925–937.

Gooseff, M. N., J. LaNier, R. Haggerty, and K. Kokkeler (2005), Determining in-channel (dead zone) transient storage by comparing solute transport in a bedrock channel–alluvial channel sequence, Oregon, *Water Resour. Res.*, *41*, W06014, doi:10.1029/2004WR003513.

Govindaraju, R. S., and B. S. Das (2007), *Moment Analysis for Subsurface Hydrologic Applications*, Springer, Dordrecht, Netherlands.

Graf, B. (1995), Observed and predicted velocity and longitudinal dispersion at steady and unsteady flow, Colorado River, Glen Canyon Dam to Lake Mead, *J. Am. Water Resour. Assoc.*, *31*(2), 265–281.

Haggerty, R., and S. M. Gorelick (1995), Multiple-rate mass transfer for modeling diffusion and surface reactions in media with pore-scale heterogeneity, *Water Resour. Res.*, *31*(10), 2383–2400, doi:10.1029/95WR10583.

Haggerty, R., S. M. Wondzell, and M. A. Johnson (2002), Power-law residence time distribution in the hyporheic zone of a 2nd-order mountain stream, *Geophys. Res. Lett.*, *29*(13), 1640, doi:10.1029/2002GL014743.

Hall, R. O., Jr., E. S. Bernhardt, and G. E. Likens (2002), Relating nutrient uptake with transient storage in forested mountain streams, *Limnol. Oceanogr.*, *47*(1), 255–265.

Hall, R. O., Jr., et al. (2009), Nitrate removal in stream ecosystems measured by ^{15}N addition experiments: Total uptake, *Limnol. Oceanogr.*, *54*(3), 653–665.

Harvey, J. W. and K. E. Bencala (1993), The effect of streambed topography on surface-subsurface water exchange in mountain catchments, *Water Resour. Res.*, *29*(1), 89–98, doi:10.1029/92WR01960.

Harvey, C. F., and S. M. Gorelick (1995), Temporal moment-generating equations: Modeling transport and mass transfer in heterogeneous aquifers, *Water Resour. Res.*, *31*(8), 1895–1911, doi:10.1029/95WR01231.

Jobson, H. E., (1997), Predicting travel time and dispersion in rivers and streams, *J. Hydraul. Eng.*, *123*(11), 971–978.

Jury, W. A., and K. Roth (1990), *Transfer Functions and Solute Movement Through Soil: Theory and Applications*, Birkhäuser, Basel, Switzerland.

Lamontagne, S. and P. G. Cook (2007), Estimation of hyporheic water residence time in situ using 222Rn disequilibrium, *Limnol. Oceanogr.: Methods*, *5*, 407–416.

Lautz, L. K., and D. I. Siegel (2007), The effect of transient storage on nitrate uptake lengths in streams: An inter-site comparison, *Hydrol. Processes*, *21*, 3533–3548.

Lee, K. K. (1995), Stream velocity and dispersion characteristics determined by dye-tracer studies on selected stream reaches in the Willamette River Basin, Oregon, U.S. Geol. Surv. Water-Resour. Invest. Rep. 95–4078, Portland, Oreg.

Lees, M. J., L. A. Camacho, and S. Chapra (2000), On the relationship of transient storage and aggregated dead zone models of longitudinal solute transport in streams, *Water Resour. Res.*, *36*(1), 213–224, doi:10.1029/1999WR900265.

Leube, P. C., W. Nowak, and G. Schneider (2012), Temporal moments revisited: Why there is no better way for physically based model reduction in time?, *Water Resour. Res.*, *48*, W011527, doi:10.1029/2012WR011973.

Luo, J., O. A. Cirpka, M. Dentz, and J. Carrera (2008), Temporal moments for transport with mass transfer described by an arbitrary memory function in heterogeneous media, *Water Resour. Res.*, *44*, W01502, doi:10.1029/2007WR006262.

Martí, E., N. B. Grimm, and S. G. Fisher (1997), Pre- and post-flood nutrient retention efficiency in a desert stream ecosystem, *J. N. Am. Benthol. Soc.*, *16*, 805–819.

McClain, M. E., et al. (2003), Biogeochemical hot spots and hot moments at the interface of terrestrial and aquatic ecosystems, *Ecosystems*, *6*(4), 301–312, doi:10.1007/s10021-003-0161-9.

Mulholland, P. J., E. R. Marzolf, J. R. Webster, D. R. Hart, and S. P. Hendricks (1997), Evidence of hyporheic retention of phosphorus in Walker Branch, *Limnol. Oceanogr.*, *42*, 443–451.

Nash, J. E. (1959), Systematic determination of unit hydrograph parameters, *J. Geophys. Res. 64*(1), 111–115, doi:10.1029/JZ064i001p00111.

Nash, J. E. (1960), A unit hydrograph study with particular reference to British catchments, *Proc. Inst. Civ. Eng.*, *17*, 249–282.

Nash, J. E., and J. V. Sutcliffe (1970), River flow forecasting through conceptual models. Part I—A discussion of principles, *J. Hydrol.*, *10*(3), 282–290.

Neuman, S., and D. M. Tartakovsky (2009), Perspective on theories of non-Fickian transport in heterogeneous media, *Adv. Water Resour.*, *32*(5), 670–680.

Niyogi, D. K., K. S. Simon, and C. R. Townsend (2004), Land use and stream ecosystem functioning: Nutrient uptake in streams that contrast in agricultural development, *Arch. Hydrobiol.*, *160*, 471–486.

Nordin, C. F., and G. B. Sabol (1974), Empirical data on longitudinal dispersion in rivers, U.S. Geol. Surv. Water-Resour. Invest. Rep. 74–20, Denver, Colorado.

Nordin, C. F., Jr., and B. M. Troutman (1980), Longitudinal dispersion in rivers: The persistence of skewness in observed data, *Water Resour. Res.*, *16*(1), 123–128, doi:10.1029/WR016i001p00123.

O'Connor, K. M. (1976), A discrete linear cascade model for hydrology, *J. Hydrol.*, *29*, 203–242.

O'Connor, B. L., and J. W. Harvey (2008), Scaling hyporheic exchange and its influence on biogeochemical reactions in aquatic ecosystems, *Water Res. Res.*, *44*(12), W12423, doi:10.1029/2008WR007160.

O'Connor, B. L., M. Hondzo, and J. W. Harvey (2010), Predictive modeling of transient storage and nutrient uptake: Implications for stream restoration, *J. Hydraul. Eng.*, *136*(12), 1018–1032.

Pachepsky, Y. A., D. Gimenez, S. Logsdon, R. Allmaras, and E. Kozak (1997), On interpretation and misinterpretation of fractal models, *Soil Sci. Soc. Am. J.*, *61*, 1800–1801.

Pachepsky, Y. A., D. Benson, and W. Rawls (2000), Simulating scale-dependent solute transport in soils with the fractional advective–dispersive equation, *Soil Sci. Soc. Am. J.*, *64*, 1234–1243.

Perumal, M., (1994), Multilinear discrete cascade model for channel routing, *J. Hydrol.*, *158*, 135–150.

Pickens, J. F., and G. E. Grisak (1981), Modeling of scale-dependent dispersion in hydrogeologic systems, *Water Resour. Res.*, *17*(6), 1701–1711, doi:10.1029/WR017i006p01701.

Pilgrim, D. H. (1977), Isochrones of travel time and distribution of flood storage from a tracer study on a small watershed, *Water Resour. Res.*, *13*(3), 587–595.

Rao, P. S. C., D. E. Rolston, R. E. Jessup, and J. M. Davidson (1980), Solute transport in aggregated porous media: Theoretical and experimental evaluation, *Soil Sci. Soc. Am. J.*, *44*(6), 1139–1146.

Ratto, M., P. C. Young, R. Romanowicz, F. Pappenberger, A. Saltelli, and A. Pagano (2007), Uncertainty, sensitivity analysis and the role of data based mechanistic modeling in hydrology, *Hydrol. Earth Syst. Sci.*, *11*(4), 1249–1266.

Rogowski, A. S. (1972), Watershed physics: Soil variability criteria, *Water Resour. Res.*, *8*, 1015–1023.

Romanowicz, R., M. Osuch, and S. Wallis (2013), Modelling of solute transport in rivers under different flow rates: A case study without transient storage, *Acta Geophys.*, *61*(1), 98–125.

Runkel, R. L. (1998), One dimensional transport with inflow and storage (OTIS): A solute transport model for streams and rivers, *U.S. Geol. Surv. Water-Resour. Invest. Rep. 98–4018*, 73 p, Denver, Colorado.

Runkel, R. L. (2002), A new metric for determining the importance of transient storage, *J. N. Am. Benthol. Soc.*, *21*, 529–543.

Runkel, R. L. (2007), Toward a transport-based analysis of nutrient spiraling and uptake in streams, *Limnol. Oceanogr. Methods*, *5*, 50–62.

Runkel, R. L., and P. J. Restrepo (1993), Solute transport modeling under unsteady flow regimes: An application of the Modular Modeling System, in *Water Management in the '90s: A Time for Innovation*, edited by K. Hon, Proc. Water Resour. Plann. Manage. Div. ASCE, Seattle, Wash.

Runkel, R. L., D. M. McKnight, and E. D. Andrews (1998), Analysis of transient storage subject to unsteady flow: Diel flow variation in an Antarctic stream, *J. N. Am. Benthol. Soc.*, *17*(2), 143–154.

Russo, D., and E. Bresler (1981), Soil hydraulic properties as stochastic processes: An analysis of field spatial variability, *Soil Sci. Soc. Am. J.*, *45*, 682–687.

Ryan, R. J., A. I. Packman, and S. S. Kilham (2007), Relating phosphorus uptake to changes in transient storage and streambed sediment characteristics in headwater tributaries of Valley Creek, an urbanizing watershed, *J. Hydrol.*, *336*, 444–457.

Sardin, M., D. Schweich, F. J. Leij, and M. Th. van Genuchten (1991), Modeling the nonequilibrium transport of linearly interacting solutes in porous media: A review, *Water Resour. Res.*, *27*(9), 2287–2307, doi:10.1029/91WR01034.

Schmid, B. H. (2002), Persistence of skewness in longitudinal dispersion data: Can the dead zone model explain it after all?, *J. Hydraul. Eng.*, *128*(9), 848–854.

Schmid, B. H. (2003), Temporal moments routing in streams and rivers with transient storage, *Adv. Water Resour.*, *26*, 1021–1027.

Scordo, E. B., and R. D. Moore (2009), Transient storage processes in a steep headwater stream, *Hydrol. Processes*, *23*, 2671–2685.

Shlesingerm, M. F., J. Klafter, and Y. M. Wong (1982), Random walks with infinite spatial and temporal moments, *J. Stat. Phys.*, *27*, 499–512.

Silliman, S. E., and E. S. Simpson (1987), Laboratory evidence of the scale effect in dispersion of solutes in porous media, *Water Resour. Res.*, *23*(8), 1667–1673, doi:10.1029/WR023i008p01667.

Sivapalan, M. (2003), Prediction in ungauged basins: A grand challenge for theoretical hydrology, *Hydrol. Processes*, *17*(5), 3163–3170.

Sokolov, I. M. (2000), Lévy flights from a continuous-time process, *Phys. Rev. E.*, *63*, 011104.

Stendinger, J. R. (1980), Fitting log normal distributions to hydrologic data, *Water Resour. Res.*, *16*(3), 455–468.

Thomas, S. A., H. M. Valett, J. R. Webster, and P. J. Mulholland (2003), A regression approach to estimating reactive solute uptake in advective and transient storage zones of stream ecosystems, *Adv. Water Resour.*, *26*, 965–976.

Torres-Quintero, E., G. Munárriz, and D. Villazón (2006), Determinación de caudal, tiempos de tránsito, velocidad y coeficiente de dispersión en el Río Bogotá, Frío y Magdalena utilizando técnicas nucleares, *Avances Invest. Ing.*, *5*, 21–31.

Valett, H. M., J. A. Morrice, and C. N. Dahm (1996), Parent lithology, surface-groundwater exchange, and nitrate retention in headwater streams, *Limnol. Oceanogr.*, *41*, 333–345.

van Mazijk, A. (2002), Modelling the effects of groyne fields on the transport of dissolved matter within the Rhine Alarm-Model, *J. Hydrol.*, *264*, 213–229.

van Mazijk, A., and E. J. M. Veling (2005), Tracer experiments in the Rhine Basin: Evaluation of the skewness of observed concentration distributions, *J. Hydrol.*, *307*, 60–78..

Van De Pol, R. M., P. J. Wierenga, and D. R. Nielsen (1977), Solute movement in a field soil, *Soil Sci. Soc. Am. J.*, *41*, 10–13.

Wagner, B. J., and J. W. Harvey (1997), Experimental design for estimating parameters of rate-limited mass transfer: Analysis of stream tracer studies, *Water Resour. Res.*, *33*(7), 1731–1741, doi:10.1029/97WR01067.

Wagener, T., L. A. Camacho, and H. S. Wheater (2002), Dynamic identifiability analysis of the transient storage model for solute transport in rivers, *J. Hydroinformatics*, *4*(3), 199–211.

Wagener, T., H. S. Wheater, and H. V. Gupta (2004), *Rainfall-Runoff Modelling in Gauged and Ungauged Catchments*, Imperial College Press, London, England.

Webster, J. R., et al. (2003), Factors affecting ammonium uptake in streams—An inter-biome perspective, *Freshwater Biol.*, *48*, 1329–1352.

Wallis, S. G., P. C. Young, and K. J. Beven (1989), Experimental investigation of the aggregated dead zone model for longitudinal solute transport in stream channels, *Proc. Inst. Civ. Eng.*, *87*(Pt. 2), 1–22.

Wondzell, S. (2006), Effect of morphology and discharge on hyporheic exchange flows in two small streams in the Cascade Mountains of Oregon, USA, *Hydrol. Processes*, *20*(2), 267–287.

Wörman, A. (2000), Comparison of models for transient storage of solutes in small streams, *Water Resour. Res.*, *36*(2), 455–468, doi:10.1029/1999WR900281.

Xia, R. (1997), Relation between mean and maximum velocities in a natural river, *J. Hydraul. Eng.*, *123*(8), 720–723.

Young, P. C. (1998), Data-based mechanistic modelling of environmental, ecological, economic and engineering systems, *Environ. Modell. Software*, *13*(2), 105–122.

Young, P. C., and S. G. Wallis (1993), Solute transport and dispersion in channels, in *Channel Network Hydrology*, edited by K. Beven and M. J. Kirby, pp. 129–173, John Wiley, Chichester, England.

Zhang, Y. and M. M. Aral (2004), Solute transport in open-channel networks in unsteady flow regime, *Environ. Fluid Mech.*, *4*, 225–247.